


2015

Development of smartphone-based spectroscopy instruments for diagnostic test analysis

Benjamin Jin Seong Ch'ng
Iowa State University

Follow this and additional works at: <https://lib.dr.iastate.edu/etd>

 Part of the [Economic History Commons](#), [Electrical and Electronics Commons](#), and the [Nanoscience and Nanotechnology Commons](#)

Recommended Citation

Ch'ng, Benjamin Jin Seong, "Development of smartphone-based spectroscopy instruments for diagnostic test analysis" (2015).
Graduate Theses and Dissertations. 14778.
<https://lib.dr.iastate.edu/etd/14778>

This Thesis is brought to you for free and open access by the Iowa State University Capstones, Theses and Dissertations at Iowa State University Digital Repository. It has been accepted for inclusion in Graduate Theses and Dissertations by an authorized administrator of Iowa State University Digital Repository. For more information, please contact digirep@iastate.edu.

Development of smartphone-based spectroscopy instruments for diagnostic test analysis

by

Benjamin Jin Seong Ch'ng

A thesis submitted to the graduate faculty
in partial fulfillment of the requirements for the degree of
MASTER OF SCIENCE

Major: Electrical Engineering

Program of Study Committee:

Meng Lu, Major Professor

Long Que

Jonathan Claussen

Iowa State University

Ames, Iowa

2015

Copyright © Benjamin Jin Seong Ch'ng, 2015. All rights reserved

TABLE OF CONTENTS

LIST OF FIGURES.....	iv
ACKNOWLEDGEMENT	vii
ABSTRACT.....	viii
CHAPTER 1 : INTRODUCTION.....	1
1.1 Mobile Health.....	1
1.2 Molecular Diagnostics	3
1.3 Organization of the Thesis	6
CHAPTER 2 : SMARTPHONE-BASED SPECTRUM ANALYZER.....	7
2.1 Background.....	7
2.2 Optical Spectroscopy Apparatus	10
2.3 Design of Transmission Setup	12
2.4 Design of Reflection Setup	18
CHAPTER 3 : CHARACTERIZATION OF THE SMARTPHONE-BASED SPECTROMETER	26
3.1 Measurement of Standard Light Sources.....	26
3.2 Analysis of the Performances.....	36

CHAPTER 4 : APPLICATION OF THE SMARTPHONE-BASED SPECTROMETER FOR SENSING	37
4.1 Background of the AAO Sensor	37
4.2 Analysis of the Performance	39
4.3 Sensing Experiments	40
CHAPTER 5 : SMARTPHONE-BASED FLUORESCENCE POLARIZATION SENSOR.....	49
5.1 Background of Fluorescence Polarization Assay.....	49
5.2 Design of the Compact Instrument.....	50
5.3 Results	53
CHAPTER 6 : CONCLUSIONS.....	54
6.1 Conclusion of Research Work	54
6.2 Suggestions of Future Work.....	55
APPENDIX. PUBLICATIONS	56
BIBLIOGRAPHY.....	57

LIST OF FIGURES

Figure 2-1: Electromagnetic spectrum.....	9
Figure 2-2: Light source (front view).....	
Figure 2-3: Light source (top view)	10
Figure 2-4: OceanOptics USB4000	
Figure 2-5: OceanOptics USB4000 components.....	11
Figure 2-6: Anodized Aluminum Oxide sample	12
Figure 2-7: Order of diffracton	
Figure 2-8: Diffraction grating spectrum orders.....	13
Figure 2-9: Schematic for transmission setup	14
Figure 2-10: Back view (v1.0)	
Figure 2-11: Front view (v1.0)	15
Figure 2-12: Side view (v1.0).....	15
Figure 2-13: Front view (v1.2)	
Figure 2-14: Back view (v1.2)	16
Figure 2-15: Side view (v1.2).....	16
Figure 2-16: Schematic of reflectance setup	18
Figure 2-17: Back view (v2.0)	
Figure 2-18: Top view (v2.0)	18
Figure 2-19: Side view (v2.0).....	19
Figure 2-20: Top view (v2.1)	
Figure 2-21: Back view (v2.1).....	20

Figure 2-22: Side view (v2.1).....	20
Figure 2-23: Front-top view (v2.2).....	21
Figure 2-24: Back top view (v2.2).....	21
Figure 2-25: Bottom view (v2.2).....	21
Figure 2-26: First Test setup for transmission spectrometer v1.0.....	22
Figure 2-27: Test setup for reflectance spectrometer (v2.2).....	23
Figure 2-28: Transmission smartphone-based spectrometer.....	24
Figure 2-29: Reflectance smartphone-based spectrometer.....	25
Figure 3-1: Broadband light source (Halogen lamp).....	27
Figure 3-2: Neon lamp spectrum (reflectance spectrometer).....	28
Figure 3-3: iPhone Neon spectrum (total and split channels).....	29
Figure 3-4: HeNe laser (543 nm & 632.8nm).....	30
Figure 3-5: iPhone HeNe laser spectrum.....	31
Figure 3-6: iPhone Neon spectrum (calibrated).....	33
Figure 3-7: Mercury spectrum.....	34
Figure 3-8: iPhone Mercury lamp spectrum.....	34
Figure 3-9: Broadband light spectrum (total & split channels for Bayer filter).....	35
Figure 4-1: Anodized Aluminum Oxide sample.....	
Figure 4-2: Schematic drawing of AAO structure.....	37
Figure 4-3: Fluidic Channel made with Parafilm and a one by three inch acrylic.....	38
Figure 4-4: AAO spectrum measured with smartphone and OceanOptics.....	39
Figure 4-5: % DMSO concentration on Photonic Crystal.....	41

Figure 4-6: Wavelength shift based on Refractive Index.....	41
Figure 4-7: Schematic of Polyelectrolyte Layers.....	43
Figure 4-8: Polyelectrolyte layers on Photonic Crystal.....	43
Figure 4-9: Wavelength peak shift as layers increases.....	44
Figure 4-10: Polyelectrolyte layers on AAO (400nm-475nm).....	45
Figure 4-11: Polyelectrolyte layers on AAO (475nm-535nm).....	46
Figure 4-12: Wavelength shift with stacked polyelectrolyte layers	46
Figure 4-13: Polypeptide on AAO sample.....	48
Figure 5-1: Schematic for Fluorescence Polarization Sensor.....	50
Figure 5-2: Top view	
Figure 5-3: Side view	51
Figure 5-4: 3D-printed Fluorescence Polarization Sensor	52
Figure 5-5: Fluorescence Polarization Sensor Image.....	53

ACKNOWLEDGEMENT

I would like to express my sincere gratitude and appreciate towards Professor Meng Lu who has provided excellent guidance, patience and vision over the two year of my graduate studies. Professor Meng Lu has always made himself available to guide me and advise me when discussing my research, different topics and most importantly, the direction of my future career.

I also express my deepest appreciation the committee members, Professor Long Que and Professor Jonathan Claussen for being a part of my program of study committee members. They are always available whenever I have questions or needed help. I would also like to thank Professor Gary Tuttle for his help as I decided to pursue my masters and advised me when I needed help.

Next, this dissertation would not have been completed if I did not have the constant encouragement from my friends and LIOS research group members. They have constantly been supporting me and creating such a wonderful environment to work in. They have made my time as I pursue my masters much more enjoyable and interesting.

Lastly and most importantly, I am most grateful and am sincerely thankful for my family that has always supported me throughout my life. Their concerns, and never-ending e has helped me through my time as a graduate student and therefore, I would like to dedicate my thesis to my family.

ABSTRACT

The latest smartphones are increasingly seen as handheld computers owing to the capabilities that are currently offered by smartphones. So far, many health related issues have already benefited from the usages of mobile health technologies and there will be certainly many more coming in the future. This research aims to advance the field of mobile health by turning the existing smartphones into a sensor readout system that is capable of measuring disease biomarkers. This thesis focuses on the development of a smartphone-based spectrum analyzer using the hardware, such as the camera, flash light, and display, of the smartphone. In conjunction with the anodized aluminum and photonic crystal sensor, the developed system measures the change in refractive index induced by the capture of biomarkers. The characterization and integration between the smartphone and spectrometer are carried out to ensure robust and reliable measurements. The smartphone-based spectrometer is able to measure accurately as compared to commercial spectrometers. The spectrometer is designed to be compact and hopefully would impact the mobile health technologies in the near future.

CHAPTER 1 : INTRODUCTION

1.1 Mobile Health

As technology improves at a rapid speed, many gadgets are getting smaller and more portable. The smartphones industry has always been competitive and constantly improving as the years go by and is even more powerful than the computer that was used to send the first man to the moon. With such a powerful device in the hands of almost two billion humans on earth, it has piqued the interest of many to see how a smartphone will be able to assist humans in various fields of life. It has definitely redefined the field of communication around the world, allowing people to communicate from different countries without any hassles.

Another field of study that is really important is medicine, where the maintaining and improving health of patients will always be the top priority. Doctors, scientists and researchers have always been working hard to find cures for diseases and improving current technology in order to treat patients efficiently and more accurately. Over the years, the smartphone technology has matured to the extent that many different kind of health apps are being developed to assist the healthcare of patients, such as collecting health data, healthcare information delivery, real-time monitoring of patients vital signs, and also direct provision care through mobile telemedicine. Thus, health information can be transferred over the internet to medical facilities which allows doctors to diagnose diseases from afar. More common diseases can be added to a “disease bank” and if the symptoms match, users will be diagnosed immediately. This not only helps

patients but is very useful discover new and rare diseases of patients that do not have access to a health facility. This is known as mobile health.

Today, mobile health has grown so much that it has become an established environment where the benefits of owning and using a smartphone are able to help deliver health information to users. Although there has been much improvement since mobile health has been known, there is still much more needed to be done in order to transmit health information for the many across the globe that have little to no access to a good medical facility. For example, I know that medical facilities in Africa are scarce and many are not able to get a diagnosis in time before the disease is terminal. With a population of 1.11 billion people, CNN states that 10% of the population are smartphone users and the number is set to double in Africa over the next 4 years. Therefore, by provided a mobile healthcare to Africans, this would drastically improve the health of the African people by allowing them to diagnose diseases and possibly get a cure much earlier. It is clear that mobile health will definitely play a huge part in third world countries where smartphones are more accessible than medical facilities.

Just in the United State of America alone, by the end of 2015, a prediction of approximately 184.2 million people will be an owner of a smartphone. That is about 10% of the predicted amount of smartphone users worldwide by the end of 2015. According to analyst firm Berg Insight, around 3 million patients worldwide at the end of 2013 were using home medical monitoring devices. Berg Insight has predicted that by 2018, 19.1 million patients will be remotely monitored by a home medical monitoring device. Imagine a world where people are able to detect and determine certain diseases

before it is too late. Therefore, as technology advances, it is clear that improving the utility of a smartphone for mobile health would be very important.

1.2 Molecular Diagnostics

Before proceeding further in depth into the smartphone-based spectrometer, let us first review the current technology available to users. In the recent iOS 8 platform, Apple has released an app, Health, which allows users to do various kinds of health monitoring. Apple incorporated a Medical ID tab that allows users to input personal information that would be helpful during an emergency. This is accessible even without unlocking the phone. Next, the Health Data tab allows users to input various health data from your weight or blood pressure to detailed elements in food. The Sources tab simply allows the integration of different existing health apps with the Health app from Apple. This allows the Health app to act as a hub for input and output of information. Although users are able to monitor certain health data, the Health app is not able to measure at a molecular level. This is a concern because one may look healthy physically but internally, one could be diagnosed with a terminal illness. Therefore, point-of-care testing technologies will be important to further develop mobile health on the smartphone platforms.

Due to a future prediction in shortage of clinical physicians, point-of-care testing will increase in demand. One essential prerequisite for point-of-care testing is having a detection instrument with criteria such as bring portable, inexpensive and able to share

data over the internet. Therefore, in order to measure at a molecular level, add-on devices to smartphones have been made to improve health monitoring. Since there is a prediction that there would be a shortage of clinical physicians, point-of-care testing will increase in demand, allowing patients to diagnose their symptoms beforehand.

One popular format of a wet-lab biochemistry assay is the Enzyme-Linked Immunosorbent Assay (ELISA). It has a rapid quantification of protein and antibodies for various diseases ranging from HIV to cancer and over 40,000 articles which involves technology annually. The objective of ELISA is to measure the concentration of an analyte (antigens or antibodies) in solution. It first begins with a coating step where an analyte is adsorbed onto a polystyrene 96-well plate. Then, blocking is done where an unrelated protein-based solution is used to cover the unbounded sites on the plate. Next, the high specificity of the antibody-antigen interaction is exploited in order to detect a colorimetric change of liquid sample based upon the cleavage of a chromogen moiety. This is where the enzyme-conjugated analyte binds specifically to a target antigen or antibody. Finally, the results can be determined by adding substrate and the signal produced by the enzyme-substrate reaction is measured. Alternatively, this can be done via interpolation by obtaining a calibration curve from known concentrations of an analyte within a test sample. Since ELISA uses a surface binding for separation, between each step, excess liquid is removed and the plate is washed in order to remove unbound materials.

Next, light microscopy is a method that is cost saving, simple and vital for diagnosis and screening of infectious diseases. However, in many parts of the world, the

required equipment needed is either unavailable, insufficiently portable, and/or operators are not able to fully utilize the images obtained. However, in these regions of the world, smartphones are popular and well served by mobile phone networks. This provides possibilities for portable smartphones to be used as diagnostic imaging and telemedicine. Light spectroscopy measures the light that is either reflected or transmitted from a material or sample. The light behaves differently for different materials. Only certain wavelengths of light will be absorbed while others get reflected. For example, when the transmission for photonic crystal is measured, there will be a dip at approximately 597nm. However, when the reflectance of the photonic crystal is measured, there will be a peak at 597nm. Therefore, we know that the light at 597nm is reflected on a photonic crystal sample.

1.3 Organization of the Thesis

Chapter 2 describes the smartphone-based spectrum analyzer. A brief background of the spectrum analyzer and optical apparatus followed by the design of the transmission and reflection based spectrum analyzer.

Chapter 3 discusses the application of the smartphone-based spectrometers. The measurement of standard light source and analysis of the performance of the smartphone-based spectrometers will be discussed.

Chapter 4 will be on the application of the smartphone-based spectrometer for sensing. The background of the Anodized Aluminum Oxide (AAO) sensor will be discussed briefly before going into the performance analysis and experiments.

Chapter 5 describes another type of smartphone-based sensing, which is a fluorescence polarization sensor. In this chapter, the background of the fluorescence polarization sensor will be explained followed by the design of the sensor and results.

Chapter 6 highlights the conclusions from this research. Directions for future work regarding the smartphone-based spectrometer and fluorescence polarization sensor are suggested.

CHAPTER 2 : SMARTPHONE-BASED SPECTRUM ANALYZER

The goal of this chapter is to get a brief review on the history of how spectrometers came about, introduce the optical spectroscopy apparatus used for my research, and then show how the spectrometer was designed differently for both the transmission and reflection setup.

2.1 Background

The term spectroscopy aroused first in 1666 when Isaac Newton successfully demonstrated white light dispersed into different colors when passing through a prism. Although producing a rainbow by a prism was known to the ancients, Newton explained that the colors did not come from the prism but were actually components of sunlight and was known as spectrum. This was how he explained it: "And so the true Cause of the Length of that Image was detected to be no other, than that *Light* is not similar or Homogienal, but consists of Difform Rays, some of which are more Refrangible than others."

There are three general types of spectra that is generally known. The first spectra is the continuous spectrum which is the most well-known spectrum to most people. This spectra exhibits all the component colors of the rainbow. Secondly, there is the dark-line spectra such as the solar spectrum and from stars. Thirdly, there is the bright-line spectra that is emitted from gas discharge tubes and certain nebulae. The behavior of the rainbow colors have proved to be so important that the study of the spectrum is known as

spectroscopy. Since then, there has been many different types of spectroscopy that were discovered over the years such as infrared spectroscopy, x-ray spectroscopy, astronomical spectroscopy, plasma emission spectroscopy and many more.

Optical spectroscopy is a type of spectroscopy where the properties of physical objects are studied based on how the object interacts and emits light. Absorption spectroscopy, emission spectroscopy and fluorescence spectroscopy all fall under the optical spectroscopy. It has become the interest of research over the years and has advanced tremendously. It first started off with early spectroscopes using prisms with graduations that mark wavelengths of light. This was before researchers found out about the diffraction grating structure. In the modern day, in order for a basic and simple spectrometer to work, there are several apparatus that are needed. First, a light source is needed. Second, some sort of device that is able to select a specific or a range of wavelengths from that light will be used. This can be something as simple as a filter or something more complex such as a monochromator or interferometer. Finally a light detector for the light source is required to detect and present the sample to the spectrometer.

Although most people tend to think of light as visible, light has a much broader spectrum than that, with a spectrum ranging from 10^{-12} meters to 10 meters. This electromagnetic spectrum ranges from long wavelength which is radio waves, to microwaves and infrared light, to visible light (which is our rainbow spectrum), to ultraviolet light, then to shorter wavelengths of x-rays, gamma rays and finally cosmic rays. This is shown in the electromagnetic spectrum in Figure 2-1 below.

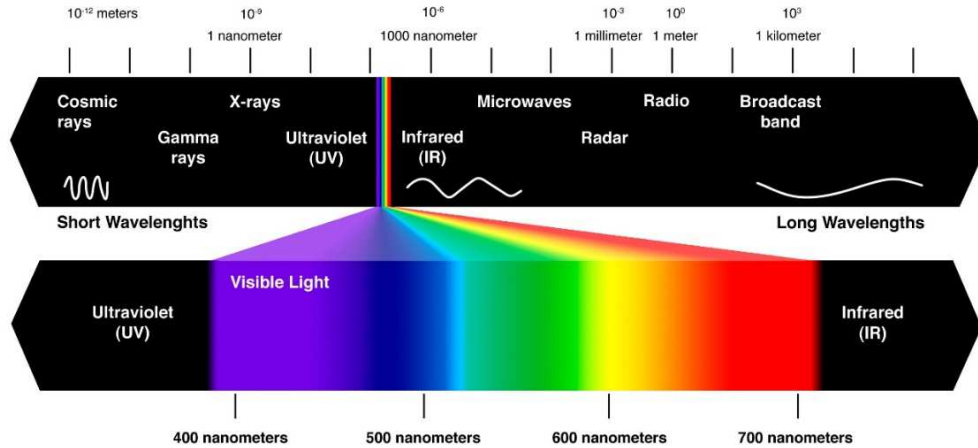


Figure 2-1: Electromagnetic spectrum

As the years have gone by, optical spectroscopy or optical imaging has become increasingly important for various fields in science. In the medical field, many are researching on optical spectroscopy as a means for further improvement of health care. As explained in [Chapter 1](#) regarding mobile health and various kinds of molecular diagnostic tests, we are capable of making portable spectrometers that will be able to produce similar results as the spectrometers in the lab. In this thesis, I will explain how I designed and made the smartphone-based portable spectrometer and tested it.

In the next section of this chapter, I will describe the optical apparatus used for testing to create a portable smartphone-based spectrometer.

2.2 Optical Spectroscopy Apparatus

Therefore, in order to further improve spectrometers, portable spectrometers that are able to do the job of a spectrometer would be essential. In [Chapter 2.1](#) I briefly explained the basic apparatus needed to make a spectrometer. In this part of the chapter, I will introduce the different optical spectroscopy apparatus I used to create and calibrate the smartphone-based spectrometer.

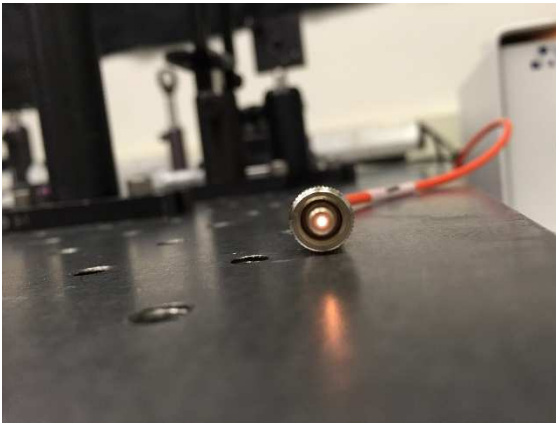


Figure 2-2: Light source (front view)

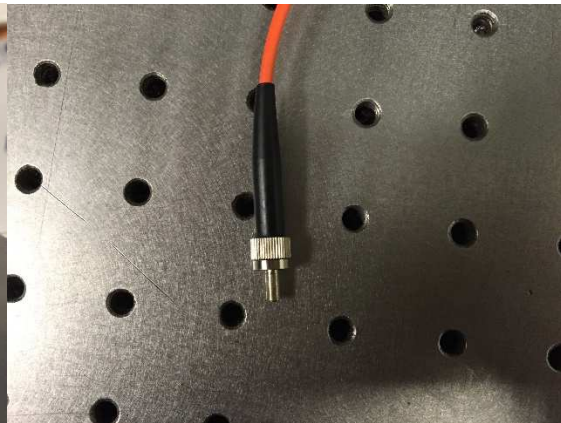


Figure 2-3: Light source (top view)

First, I have a halogen lamp that is connected to a fiber optics wire (Figure 2-2) which collimates the light beam and produces a small pin-hole light beam. This is the broadband light source used for almost of the experiments that were conducted.



Figure 2-4: OceanOptics USB4000



Figure 2-5: OceanOptics USB4000 components

OceanOptics is a company in the field of optical measurement technologies that is well known for their spectroscopy devices. Since it is so well known, many of their devices have been used for research in various fields of optics. Likewise, in order to ensure that the measurements are accurate and correct, I used an OceanOptics spectrometer as a referral during the initial stage of measurements. The spectrometer model that was used for the measurements was an Ocean Optics USB4000 (Figure 2-4). The USB4000 is able to measure from 400nm to 1000nm with a diffraction grating groove density is 1200. The groove density is important because it results in a greater dispersion and higher resolution with a higher groove density. Having more lines per mm means that the spectrometer would be able to have higher resolution capabilities.

Therefore, the USB4000 was used for calibration and ensuring that the measurements and results made by the smartphone-based spectrometer is reliable.

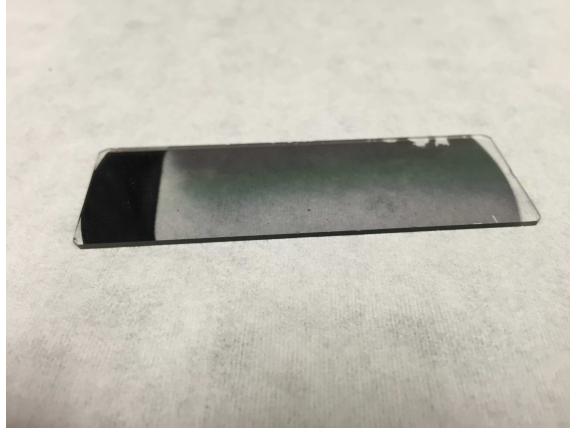


Figure 2-6: Anodized Aluminum Oxide sample

In the figure above, the Anodized Aluminum Oxide (AAO) sample that was provided by Professor Long Que and Yuan He was used for testing. AAO is a highly porous array nanostructure. Further details of this sample will be discussed in [Chapter 4](#).

2.3 Design of Transmission Setup

In this section, I will discuss the transmission spectrometer that I made. The transmission setup was our first version of the spectrometer. In this setup, I started by testing the paper-based spectrometer that was made out of card stock paper. However, the paper based setup was not robust enough and albeit producing a spectrum of light, the spectrum was not good enough for measurements. However, I do believe that the paper-based spectrometer is very useful to teach someone that is learning what is a

light diffraction and spectrum. Therefore, in order to start on creating a robust and reliable spectrometer, I did some brainstorming with Professor Meng Lu. After much discussion, I decided to take the route of 3D-printing the spectrometer. Firstly, the design was sketch roughly and then I proceeded to using Solidworks to make a better sketch model that could be seen from all angles. For this first design, which is the transmission design, I chose to attempt to obtain the first order of diffraction from the grating structure. Therefore, after some calculations and comparison to the card stock paper spectrometer, I decided to design the smartphone-based spectrometer with a slant of approximately 47° angle.

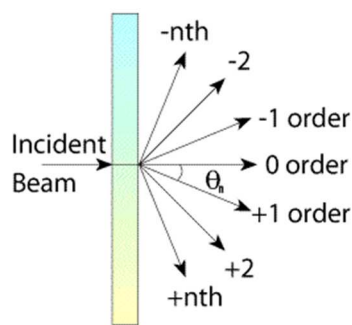


Figure 2-7: Order of diffraction

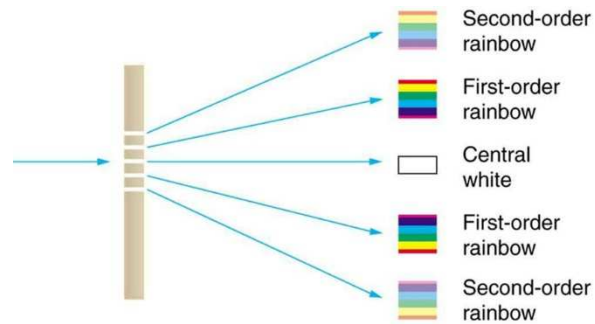


Figure 2-8: Diffraction grating spectrum orders

As shown in Figure 2-7 above, the first order diffraction of the grating structure is about $\sim 45-47^\circ$ angle from zero order. Therefore, in Figure 2-7, the first order diffraction produces a define spectrum. Due to this being a transmission based spectrometer, the only way to get light was to make the spectrometer extrude out of the phone. This can be seen in the schematic drawing (Figure 2-9) below.

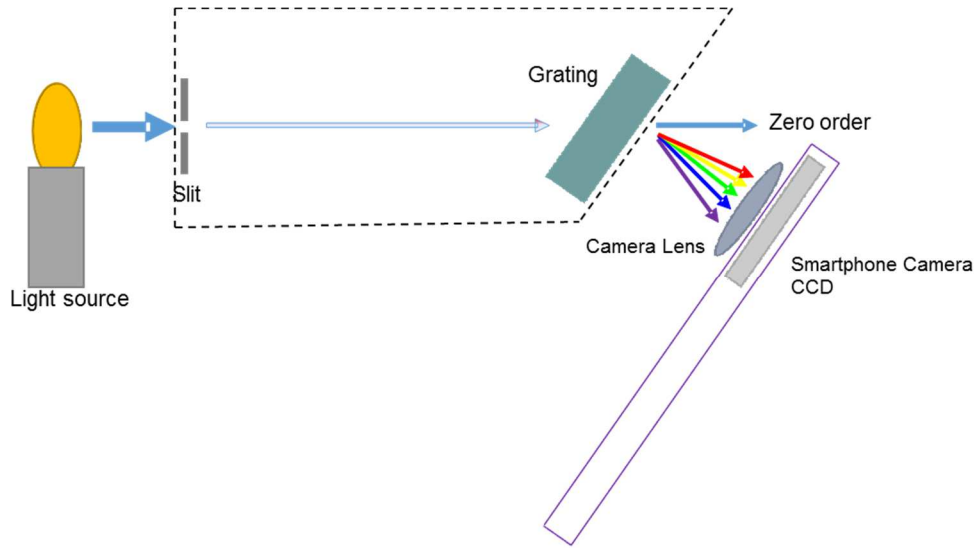


Figure 2-9: Schematic for transmission setup. Light emission from the lamp enters the spectrometer via a slit. The grating is placed on the other end of the spectrometer to diffract light. The first order of diffractions are measured using the smartphone camera.

In the schematic drawing for the transmission setup (Figure 2-9), the light source provides a beam that travels and falls upon the slit where only a certain amount of light is allowed through. The light then travels through a pass that will hit the diffraction grating. Then, the transmission grating structure will disperse the light according to the different wavelengths of color respectively. The first-order diffraction falls onto the camera lens of the smartphone and is focused onto the smartphone camera's Charged Coupled Device (CCD).

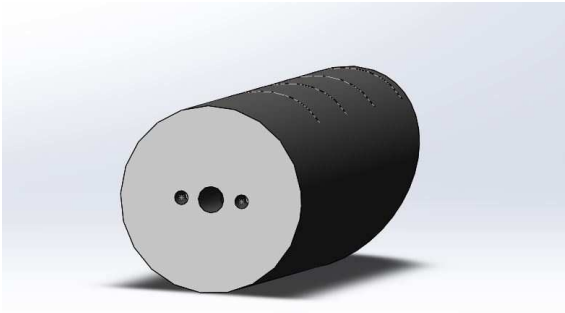


Figure 2-10: Back view (v1.0)

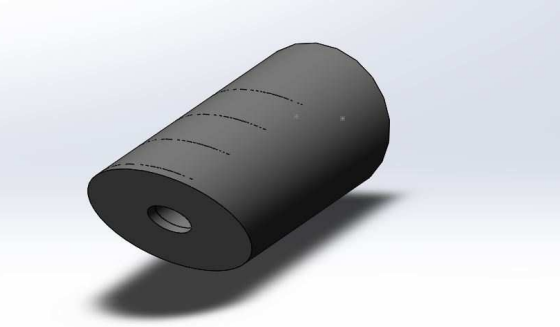


Figure 2-11: Front view (v1.0)

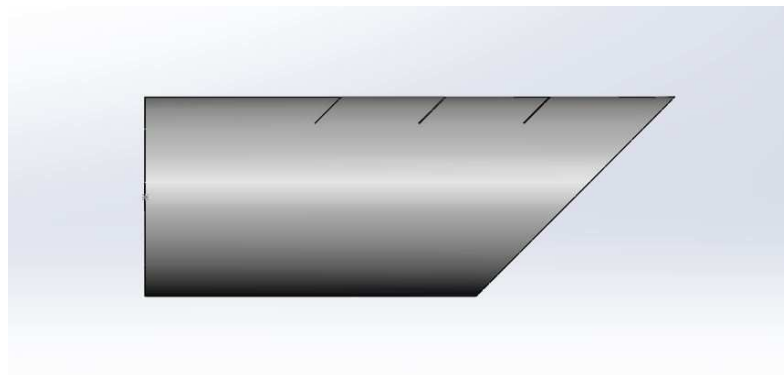


Figure 2-12: Side view (v1.0)

The very first design for the smartphone-based spectrometer is shown in the three figures above (Figure 2-10 to 2-12). Three openings on the top of the spectrometer were made at different distances from the camera CCD for diffraction grating to be inserted. This would allow for more testing with the spectrometer if the distance of the grating was either too close or too far from the camera CCD. The diffraction grating used for this first version had 600 lines/mm. Thus, this made the spectrum not as sharp and clear. Since this was the first ever version of the

spectrometer, there was much that could still be improved. Several adjustments were made and as the adjustments were done, different versions started appearing that will be shown as and discussed. As this was just the first design test, it was not able to be attachable to smartphones. This was immediately fixed in the following version. Thus, we proceeded to designing version 1.2.

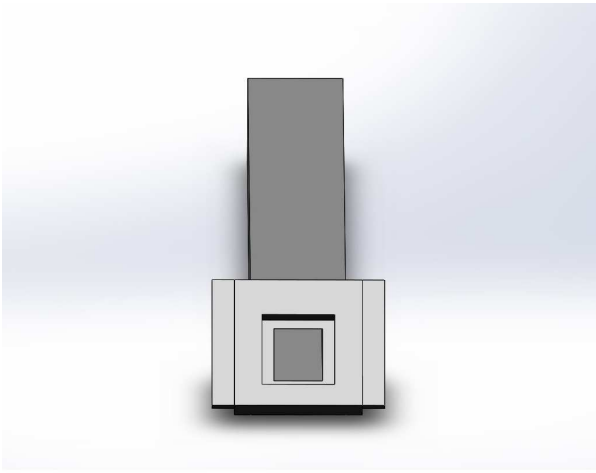


Figure 2-13: Front view (v1.2)

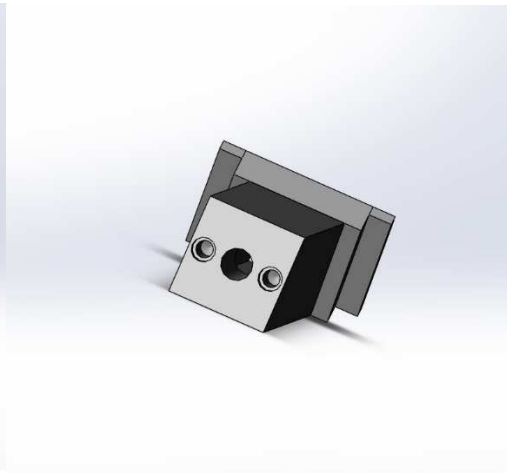


Figure 2-14: Back view (v1.2)

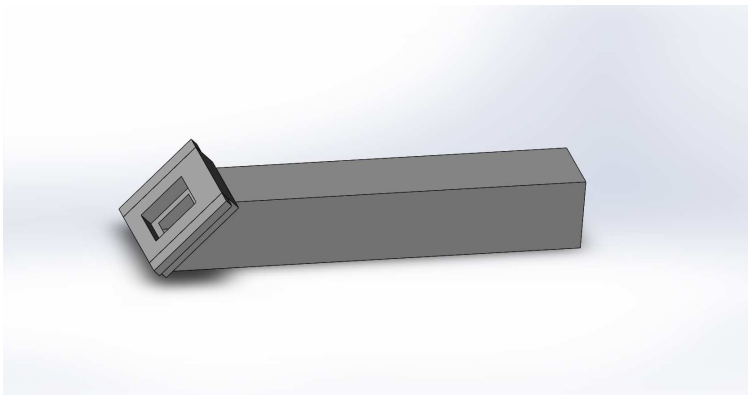


Figure 2-15: Side view (v1.2)

Version 1.2 is a more refined design of the transmission setup for the smartphone-based spectrometer. In this design, the spectrometer was made more compact and is also attachable to the smartphone. However, in order to not stick it directly onto the smartphone, we attached it onto a smartphone cover instead. That way, the spectrometer can be removed at any time and it would not damage the smartphone. In version 1.2, I changed the diffraction grating which has increased the lines from 600lines/mm to 1200lines/mm. By doing so, a much better resolution was obtained and the spectrum was sharper in color. As seen in the figures above (Figure 2-13 to 2-15), the grating structure is placed in the pocket shown in Figure 2-13 and then the spectrometer is attached to a smartphone cover so that the position of the grating will not shift. Although the spectrometer is attachable, it still extrudes out of smartphone and is not as compact as intended. After some discussion, Professor Meng Lu and I believed that the portable spectrometer can be improved further. We considered a reflection based spectrometer which would be parallel to the smartphone and found that it was feasible. Therefore, I proceeded towards designing a reflection based spectrometer.

2.4 Design of Reflection Setup

After some calculations and calibrations were made with the transmission spectrometer to ensure that the design of the optical pass and spectrometer was working well, I decided to pursue a reflectance based spectrometer.

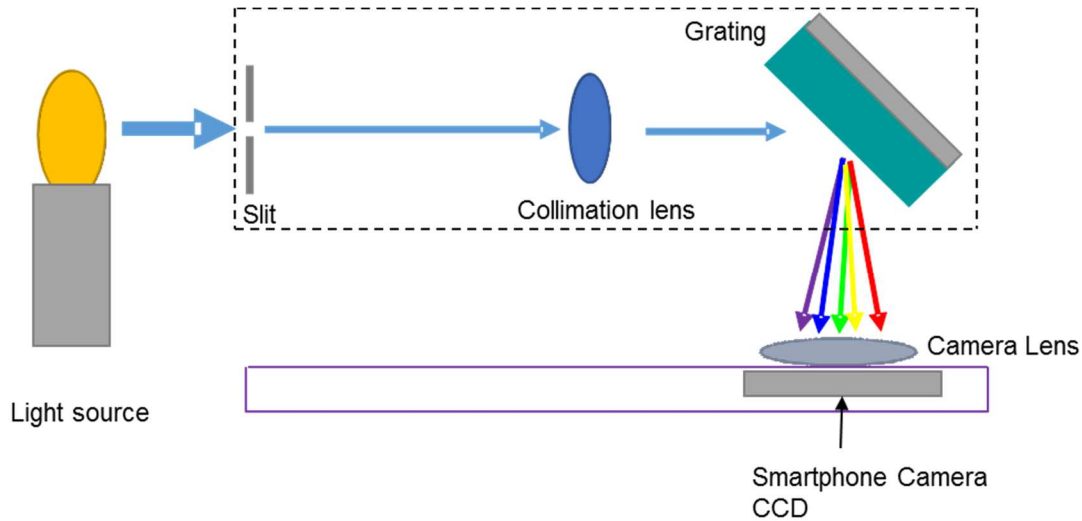


Figure 2-16: Schematic of reflectance setup. Light emission from the lamp enters the spectrometer via a slit. The grating is placed on the other end of the spectrometer to reflect and diffract light. The first order of diffractions are measured using the smartphone camera.

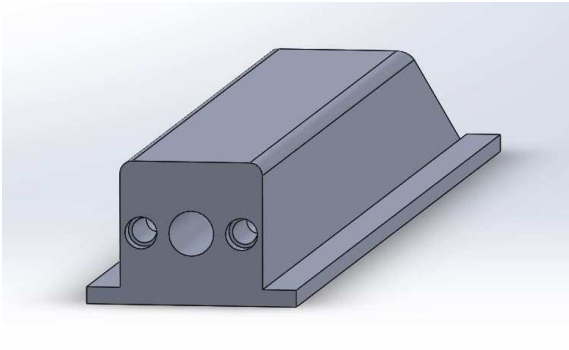


Figure 2-17: Back view (v2.0)

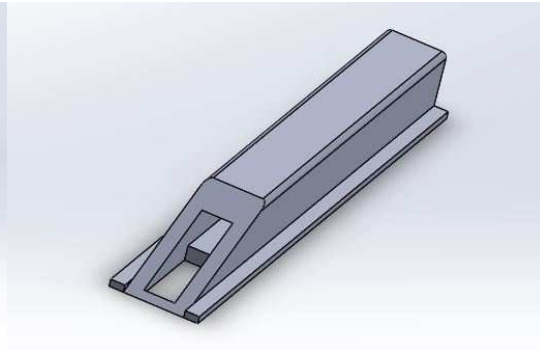


Figure 2-18: Top view (v2.0)

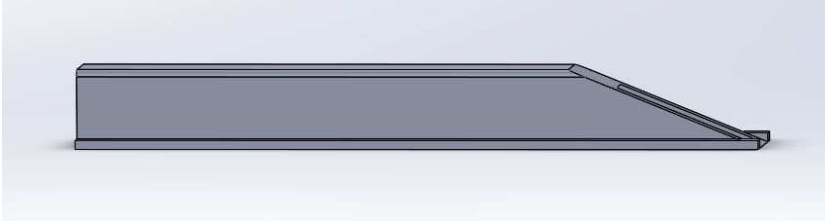


Figure 2-19: Side view (v2.0)

After going through the schematic (Figure 2-16), I used Solidworks to start designing the reflectance version. This first version of the reflectance-based spectrometer was designed quickly for testing so that adjustments could be made to improve the spectrometer. Since this is different from the transmission setup, I decided to test the angle (68° degrees) that the reflection grating would be able to reflect the first-order spectrum right onto the CCD of the smartphone camera. In the schematic shown above (Figure 2-16), the optical pass is similar to the transmission setup. However, note that the diffraction grating is placed differently. With this setup, the spectrometer was able to be more compact as it would lay parallel to the smartphone.

In the design sketches (Figure 2-17 to 2-19), the diffraction grating had to be stuck onto the slope (Figure 2-18) because the exact position for the grating was yet to be determined and there was no pocket for the grating to be dropped into. This was one of the adjustments that had to be made in order to make the spectrometer robust. Once the average position for the grating was determined, I started sketching the next version in order to improve the spectrometer.

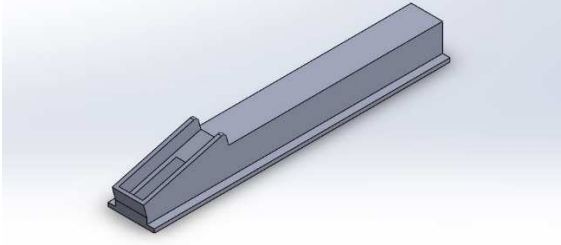


Figure 2-20: Top view (v2.1)

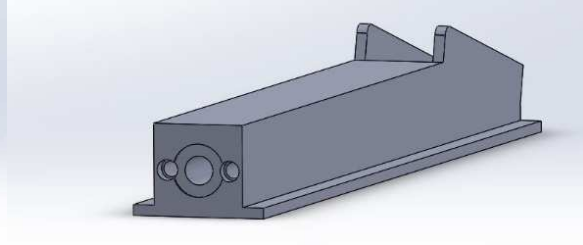


Figure 2-21: Back view (v2.1)



Figure 2-22: Side view (v2.1)

Version 2.1 is really similar to version 2.0 with several improvements. First, a pocket was made so that the diffraction grating structure would be able to be more stable even if the smartphone was moving. This meant that it would not need to be stuck onto the slope but could sit perfectly because it was made to fit the grating structure. Next, I changed the slope angle from 68° to 75° degrees. This allows the reflection grating to direct the light straight onto the camera CCD without having to move the spectrometer to fix the optical path. Furthermore, the back of the spectrometer has been modified to allow the slit to be inserted without the two pin holes and was done in attempt to make the spectrometer more compact. I managed to determine that the grating structure should be placed right at the end of the front of the

spectrometer. The results of this spectrometer was great and I wanted to add a collimation lens in so I proceeded to version 2.2.

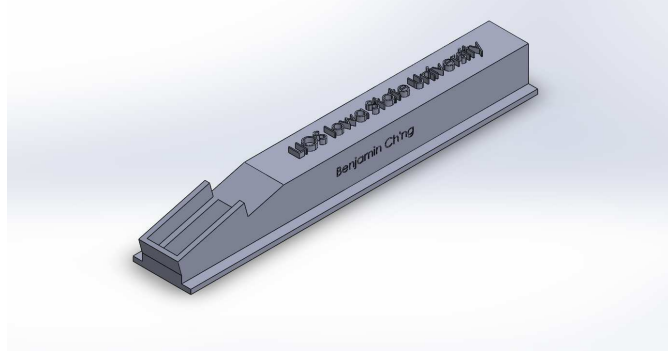


Figure 2-23: Front-top view (v2.2)

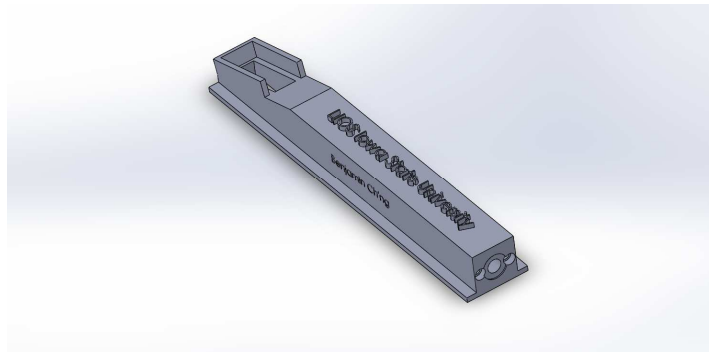


Figure 2-24: Back top view (v2.2)



Figure 2-25: Bottom view (v2.2)

In version 2.2 of the reflectance setup, I did slight modifications to the spectrometer. Firstly, I shorten the length of the pocket in the front to fit the diffraction grating better. I also added three slots for the collimation lens. I measured the distance of each slot according to the collimation lens that Professor. Lu provided.

After testing both transmission and reflection based spectrometers, I found that the reflection based spectrometer produced a higher resolution spectrum. Besides that, the reflectance-based spectrometer is much more compact than the transmission-based spectrometer. Therefore, from here on out, I proceeded with the reflectance-based spectrometer for all experiments and measurements.

Before moving on to the next chapter, where I will discuss the characterization of the smartphone-based spectrometer, I will show the setup created for testing in the lab.

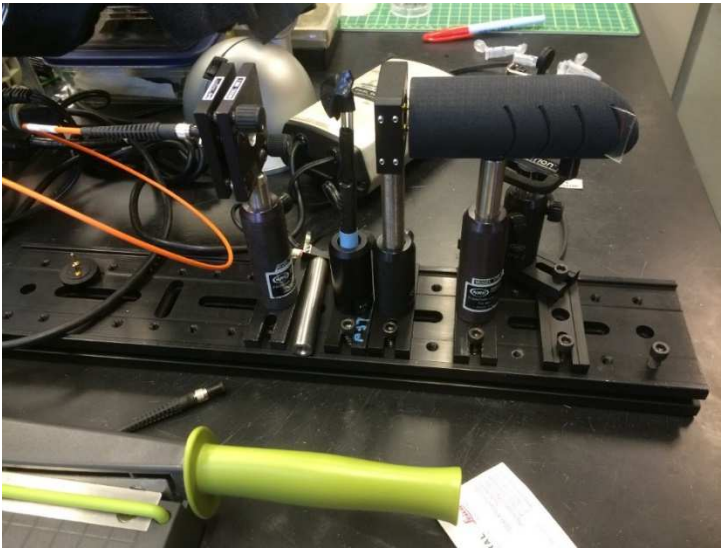


Figure 2-26: First test setup for transmission spectrometer v1.0. Schematic for the transmission setup was proven to work with this testing. Further improvements and testing were done for the transmission spectrometer.

In Figure 2-26, the setup is made for v1.0 of the transmission-based spectrometer where the spectrometer is not able to be connected to the smartphone and is a separate device. In this setup, the light source is shone straight onto the slit where the spectrometer is mount upon with two pins. The smartphone is mounted onto the smartphone holder and the phone is angled where the camera lens would be placed right where the first-order diffraction of light would fall upon. However, this was just the start of testing. For version 1.2 of the transmission spectrometer, the spectrometer was integrated with the smartphone. This is shown in the figure below. As explained earlier, we did not do much measurement testing on this spectrometer because it extrudes out of the smartphone and the resolution was not as good. Now, let us take a look at the reflectance-based setup.

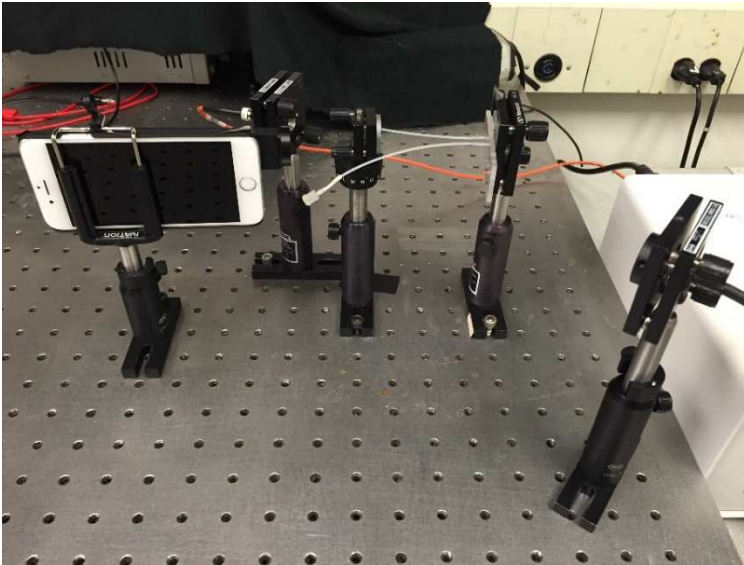


Figure 2-27: Test setup for reflectance spectrometer (v2.2). This setup was used for all the sensing experiments. Results were consistent and spectrometer was robust.

In the setup for the reflectance spectrometer, the spectrometer is integrated with the smartphone where it is mounted on the smartphone holder. The light source will shine onto the sample where there will be an angle in order for the light path to be directed right onto the slit on the spectrometer. A mirror will be placed in between the sample and spectrometer in order to reflect the light onto the detector of the OceanOptics USB4000.

After the optical setup was stable and the spectrum from the first-order diffraction was defined and had good resolution, I proceeded to the characterization of the smartphone-based spectrometers. This will be discussed in the next chapter.

Before I proceed to the next chapter, I will show you several pictures of the final products of both the transmission and reflectance based spectrometers.



Figure 2-28: Transmission smartphone-based spectrometer. This was the final version for the transmission spectrometer made. This version provided good results but we proceeded with the reflectance spectrometer due to better results.



Figure 2-29: Reflectance smartphone-based spectrometer. This was used for testing and has potential to be improved further.

In Figure 2-28, there are two pictures that show the final product of the transmission smartphone-based spectrometer. This was stuck onto the smartphone cover because there was no more improvements that will be done to the transmission spectrometer because we have decided to go forward with the reflectance spectrometer.

On the other hand, figure 2-29 shows the reflectance spectrometer. In the picture taken, there are black tapes that are visible because for the reflectance based spectrometer, there is more room for improvement that will be discussed in [chapter 6](#). Therefore, the pin slit is still used and the spectrometer can still be detached from the smartphone cover.

CHAPTER 3 : CHARACTERIZATION OF THE SMARTPHONE-BASED SPECTROMETER

This main focus of this chapter will be describing the calibration of the smartphone-based spectrometer by doing characterization of different light sources. First, the measurement of standard light sources will be discussed and then the analysis of the performance will be explained. This is an essential step in making the smartphone-based spectrometer because it will determine how well the spectrometer will work for sensing experiments in the later chapter.

3.1 Measurement of Standard Light Sources

Now that the spectrometer is robust and able to obtain a good spectrum of light when a picture is taken using the smartphone, there was still much to be done in order for it to be able to be used for measurement tests. Therefore, in order to ensure that the spectrometer is working correctly, we gathered several different light sources that would be used for testing. For this purpose, we measured broadband light, a Neon lamp a green He-Ne laser at 543nm and a red He-Ne laser at 632.8nm. The USB4000 spectrometer from OceanOptics was used to calibrate the reflectance-based spectrometer. Once this was done, the next thing I had to worry about was ensuring that the results would be uniform and able to be understood by everyone easily. For now, I will start by discussing the measurement of standard light sources.

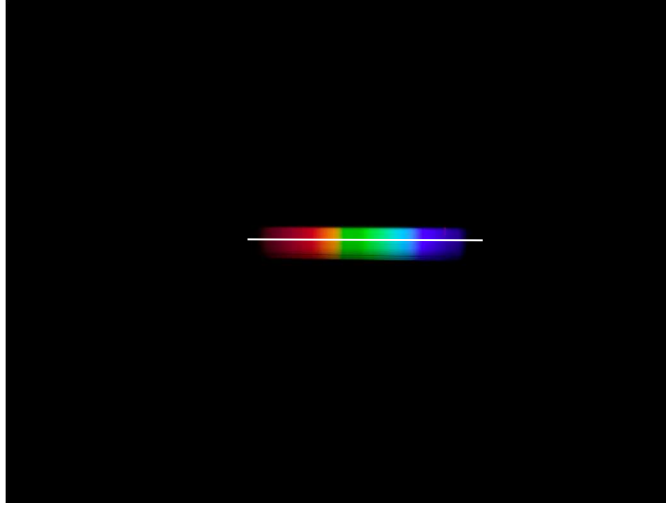


Figure 3-1: Broadband light source (Halogen lamp)

The first figure presented in this section is a picture of a broadband light spectrum taken with the reflectance-based spectrometer that was mounted onto the smartphone. This is also known as white light and Figure 3-1 above is the first-order diffraction of the light. In order to analyze the picture, the data of the spectrum is obtained by drawing a line across the spectrum. As observed in Figure 3-1, a white line is drawn across the spectrum. The white line has coordinates that will be taken down. The reason for this is because when analyzing other pictures, we want to make sure that the line drawn across the spectrums would be at the same point for each spectrum. Note that this is simply a representation of how it is done in a program called ImageJ. If we attempt to obtain an average of the spectrum, several lines are taken and the average is taken from there. ImageJ will then give an output graph of the intensity of light against the pixel number. The spectrum shown above is used as a reference for most of the measurements that will be explained in the latter chapters. Next, let us take a look at

the calibration of the spectrometer based on the different light sources that will be explained below.



Figure 3-2: Neon lamp spectrum (reflectance spectrometer)

After getting a good spectrum of the white light, I proceeded on to measuring a Neon lamp. This is shown in the figure above which represents the Neon lamp spectrum. As we observe in Figure 3-1 and 3-2, the spectrum of light is reversed as the blue wavelength is the shorter wavelength and red is longer. When we plot the graphs in respect to pixel number, the longer wavelength is the lower pixel number. This is important to be noticed because the graphs would be wrong otherwise.

Since the spectrometer has yet to be calibrated, all the data that are obtained from the pictures taken are plotted in respect to pixel numbers. This will be shown below in the Neon spectrum graph. Also, another thing to note is that as we observe in Figure 3-1 and 3-2, the spectrum of light is reversed as the blue wavelength is the shorter wavelength and red is longer. When we plot the graphs in respect to pixel

number, the longer wavelength is the lower pixel number. This is important to be noticed because the graphs would be wrong otherwise.

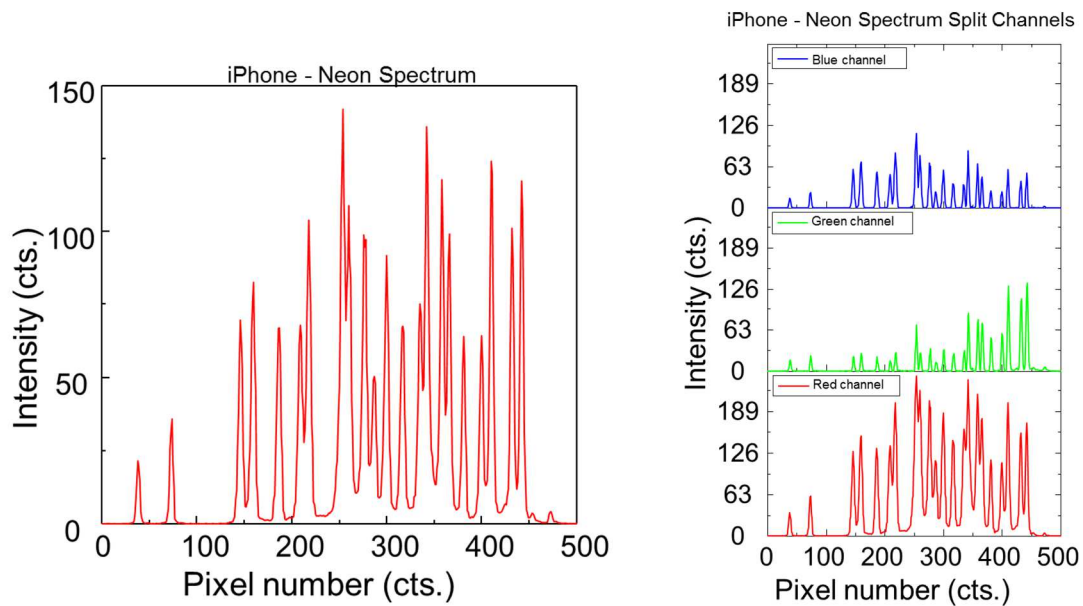


Figure 3-3: iPhone Neon spectrum. The left graph is the raw data obtained from the Neon image. The three images on the right represents the split channels from the raw data obtained. This was done using ImageJ.

As mentioned in the previous paragraph, we can observe that the x-axis on the graphs is plotted in pixel number. Both the graphs in Figure 3-3, are of the Neon spectrum before any calibration. When the peaks in the left graph are plotted AND compared to how a Neon spectrum should look like, the peaks intensity is way too high for certain peaks. This has been calibrated and will be shown later in this chapter. Although the picture is reversed, I still needed to calibrate the spectrometer in order to show a graph where the red wavelengths would be the longer wavelengths. This is

important in the future, users would not have to worry about this problem. Therefore, I proceeded to use two different lasers in order to convert pixel number to wavelength.

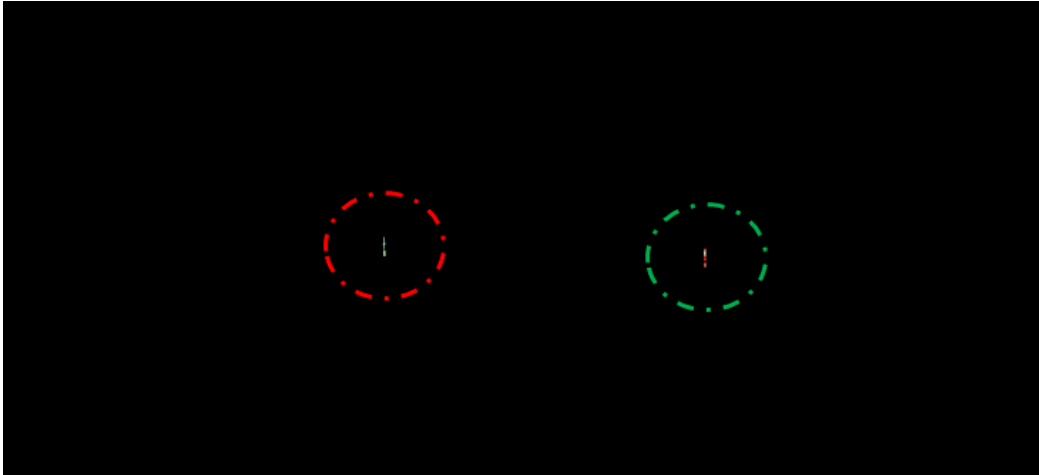


Figure 3-4: HeNe laser (543 nm & 632.8nm). The laser image circled in red represents the 543nm laser while the green circled laser image represents the 632.8nm laser.

Before I was able to get a good measurement of the laser, I had to reduce the intensity of the laser because both the lasers that were in the lab were really strong. Therefore, I had to put a filter in front of the laser to reduce the intensity. After several configurations, I managed to observe a spectrum that was not saturated by the high intensity of the lasers sharp and narrow line that I was expecting to see when measuring the lasers. The two lasers that were used are a green HeNe laser at 543nm and a red HeNe laser at 632.8nm. These pictures were taken using the smartphone-based reflectance spectrometer and we were able to observe a very sharp line for both the lasers. The green HeNe laser is encircled by red and red HeNe laser by green. As explained earlier, the same coordinates has to be used when obtaining the spectrum

data with ImageJ. This step is important because in order to convert pixel number to wavelength, both the data extracted from the spectrum needs to be starting from the same coordinate on ImageJ. After that, the data abstracted from the lasers spectrum was used to convert pixel number to wavelength using a formula. I identified the two peaks and managed to obtain the wavelengths I was expecting to get. In Figure 3-5 below, the x-axis is not plotted in terms of wavelength because the conversion was successful.

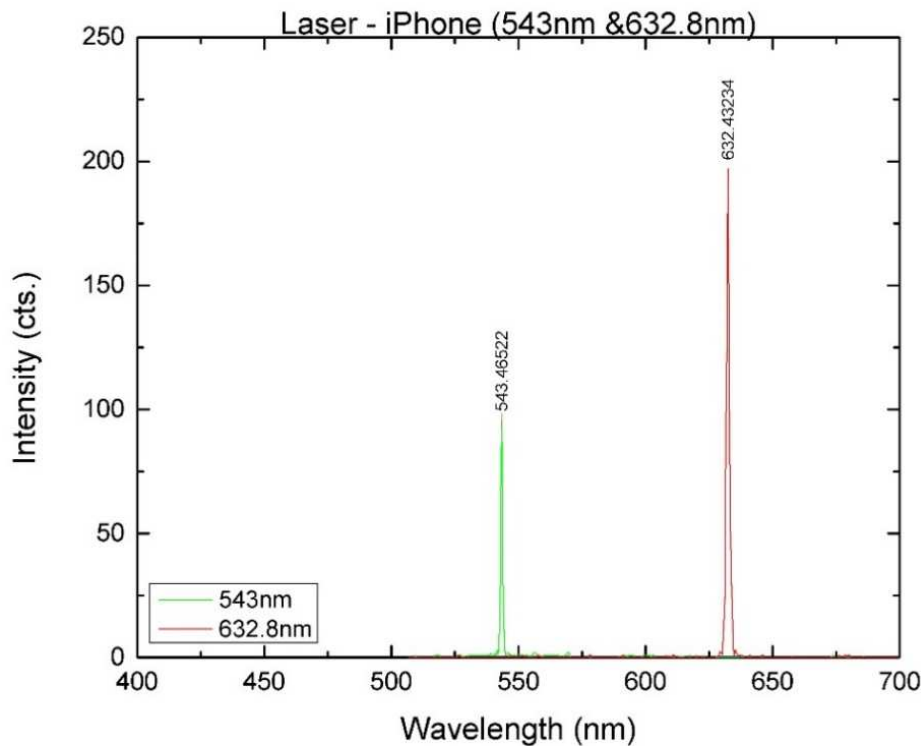


Figure 3-5: iPhone HeNe laser spectrum. As observed the lasers measured with the smartphone provided a very sharp peak.

The formula I used has been used by various companies to convert their commercialized spectrometers pixel number to wavelength. The formula is as such:

$$\lambda_p = I + C_1P + C_2P^2$$

Where, λ_p = Wavelength of pixel p, I = Wavelength of pixel 0 and C_1 and C_2 are the first and second coefficient respectively. In order to obtain the wavelength, I had to create simultaneous equations to solve for C_1 and C_2 . After solving for both, the formula was pretty straight forward and I was able to convert pixel number to wavelength easily. The Neon spectrum was replotted with respect to wavelength and is shown below. However, since the Neon spectrum had a larger wavelength range, I decided to then use the Neon spectrum as a calibration base for the future measurements I conducted. The main reason is because I was able to identify more peaks and also that I would essentially obtain wider range of wavelengths in the end. Besides that, I also found out that after converting pixel number to wavelength, I did not have to do anything to reverse the plot. Instead, the x-axis on the graph was plotted with respect to wavelength and I did not need to further calibrate the graph.

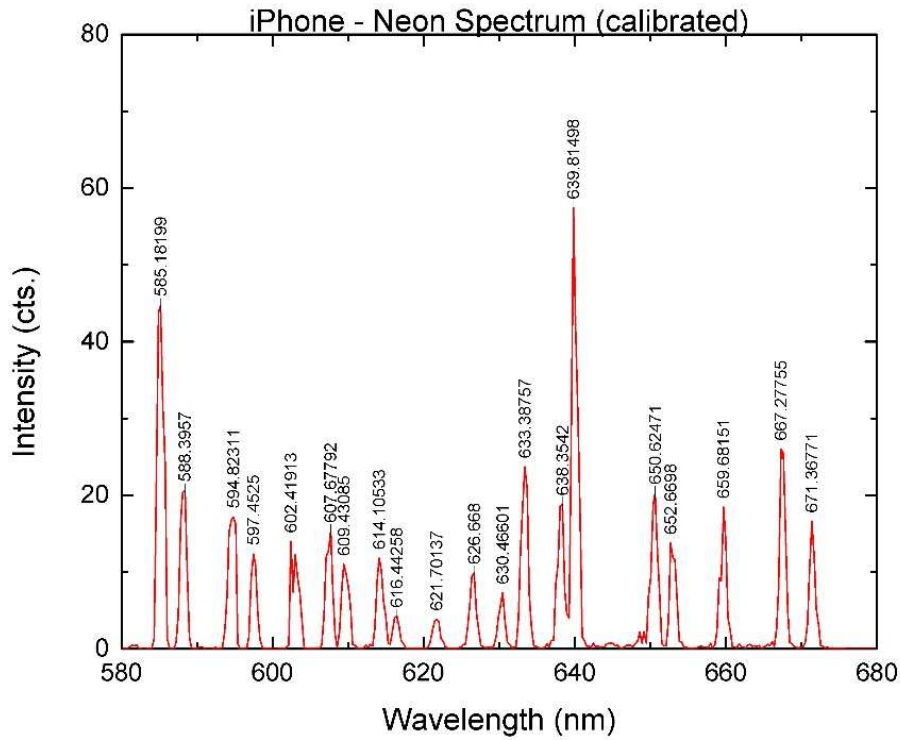


Figure 3-6: iPhone Neon spectrum ranging from 580nm to 680nm. The Neon spectrum has been calibrated.

Below, I have included a picture of a Mercury lamp to show that the spectrometer is capable of measuring different light sources accurately. Once again, the picture of the Mercury spectrum is reversed when compared to the graph in Figure 3-8. Being able to measure the Mercury lamp has simply confirmed and established that the smartphone-based spectrometer is able to measure accurately.

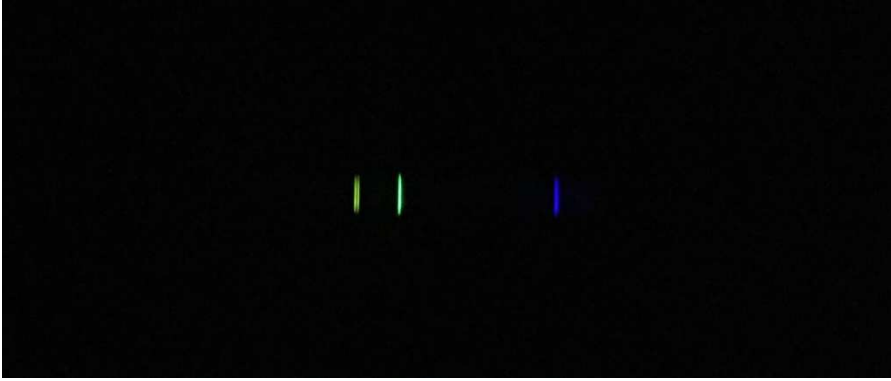


Figure 3-7: Mercury spectrum

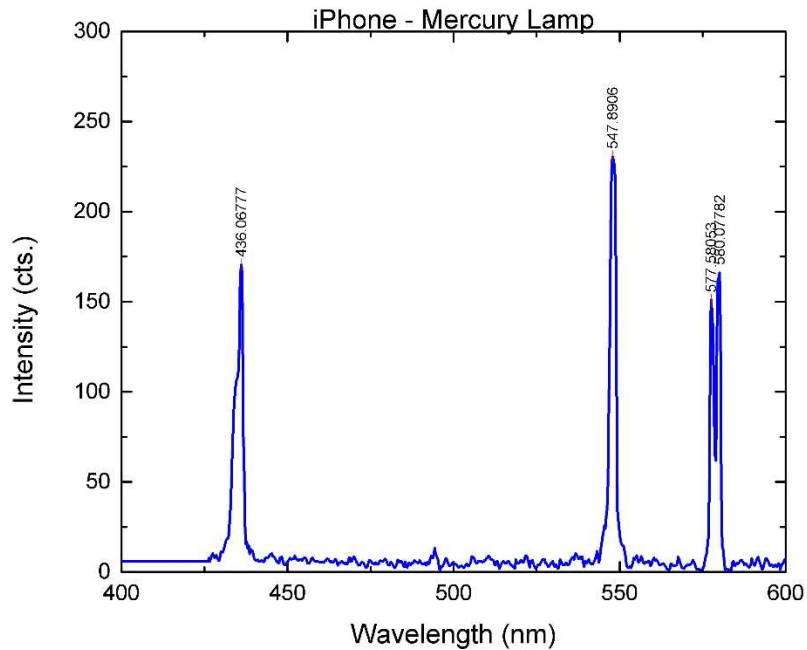


Figure 3-8: iPhone Mercury lamp spectrum

During calibration of the Neon lamp, I realized that the smartphone I was using, iPhone 6, had a few filters. After researching further, I found that the smartphone camera had a Bayer filter and an infrared (IR) filter. This caused the spectrum at approximately 650nm to be slowly cut-off disallowing any light to be measured since IR

wavelength is past 700nm. The Bayer filter on the other hand, has two green pixels for every red and blue pixel. The resolution is improved because of the filter but the exchange is that there is a certain calibration that has been done to the spectrum of the white light. This is shown below in Figure 3-9 below.

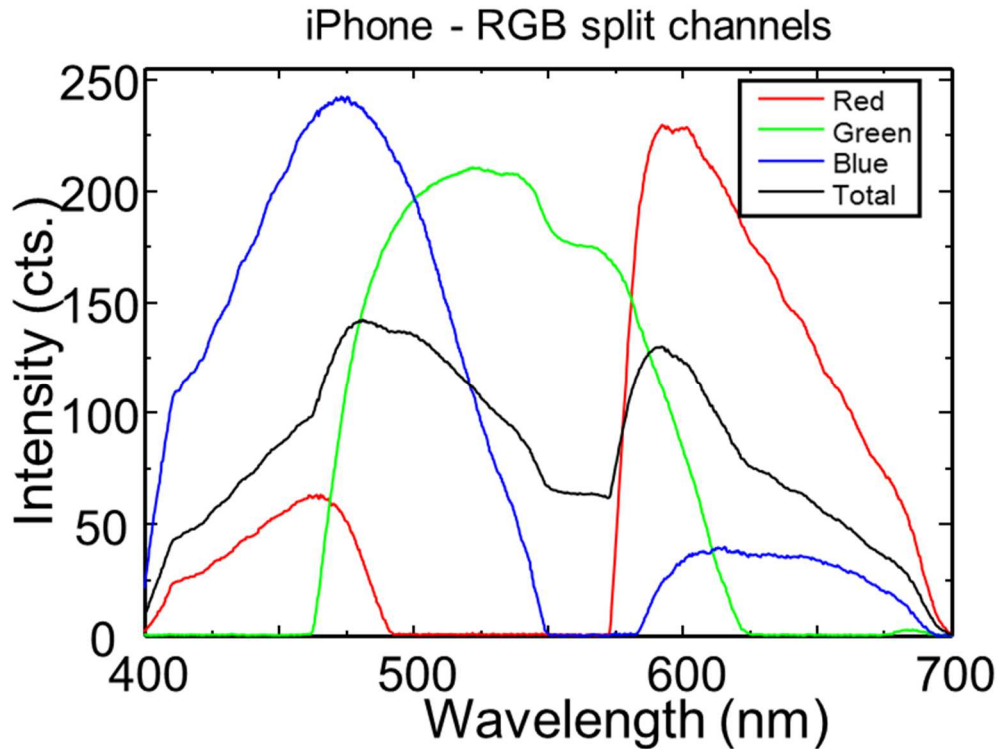


Figure 3-9: Broadband light spectrum (total & split channels for Bayer filter). This data was obtained by splitting the channels and plotting the raw data.

With the different light sources shown above, I was able to successfully calibrate the smartphone-based spectrometer. This was accurate to about approximately 1nm or 2nm for the wavelength calibration. As of now, I still have not been able to figure out a way to remove the IR filter. After some research, I believe that removing the calibration

of the Bayer filter may be possible. However, I may leave this to future work because it will take some time to figure out the intense calculations needed.

3.2 Analysis of the Performances

After I successfully calibrated the smartphone-based spectrometer, I proceeded to check the performance analysis of the spectrometer. Firstly, I managed to find out that the smartphone camera, in my case, iPhone, has different filters. There is the infrared filter that disallows any infrared light to be detected after a certain wavelength (approx. slightly after 620nm onwards) and a Bayer filter. Furthermore, after much testing, I found out that the range of the spectrometer is within the visible light range, ranging from 400nm to 700nm.

Besides that, the spectral resolution was determined to be 0.5nm while the pixel resolution of the spectrometer was 0.292654. This was all calculated using the laser spectrum as the peaks were the narrowest. All the measurements were done with a slit size of 50um.

Now that we have a working spectrometer, let us proceed to the next chapter of the thesis where I will be discussing the applications for the smartphone-based spectrometer.

CHAPTER 4 : APPLICATION OF THE SMARTPHONE-BASED SPECTROMETER FOR SENSING

Before moving on to the applications of the smartphone-based spectrometer, I will first discuss the background of a sensor that has been provided to Professor Meng Lu and me by our collaborators. After that, I will proceed to discuss about the analysis of the sensor and then finally I will proceed to the sensing experiments that I have done using the smartphone-based spectrometer.

4.1 Background of the AAO Sensor



Figure 4-1: Anodized Aluminum Oxide sample

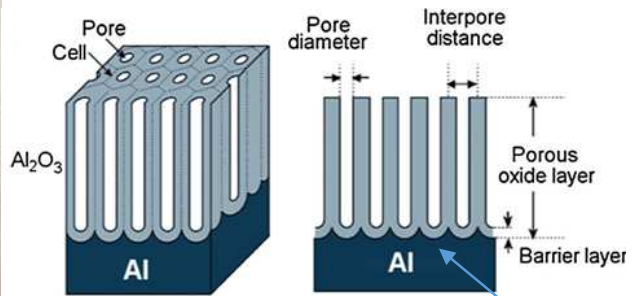


Figure 4-2: Schematic drawing of AAO structure

Hemispherical layer

Anodized Aluminum Oxide (AAO) is a close-packed hexagonal array of parallel cylindrical nanopores. Usually, these pores would lay on top of an Aluminum (Al) substrate. In this AAO sample that was provided by Professor Long Que and Yuan He, the AAO underwent a two-step anodization process. First, Al will be deposited on top of a glass slide. Next, the first-step anodization will form an Al layer that will grow over a

period of time. The alumina layer that was formed during the first-step anodization is completely etched away and nanopores will form from the hemispherical layer that is shown in Figure 4-2. The nanopores that are formed in the second-step anodization are essentially new nanopores that initiated from the hemispherical layer and is much more uniformed. Thus, the sample given is a highly porous structure.

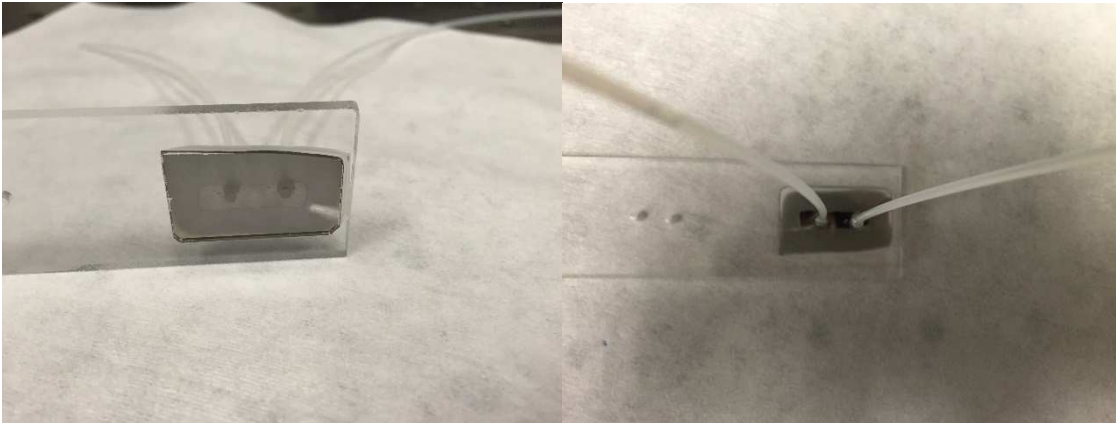


Figure 4-3: Fluidic Channel made with Parafilm and a one by three inch acrylic window

Before we started testing, in order to be efficient and save as much of the sample as possible, the sample was cut into several pieces. This can be seen in Figure 4-3. Before proceeding to the testing stage, a fluidic channel or flow cell was made using the AAO sensor. I made the flow cell by using Parafilm that would act as the adhesive layer between a 1 by 3 inch acrylic window and the AAO sample. The remaining pieces of the sample was made into two other flow cells to keep as a spare. Two holes for tubes to be connected to the flow cell were drilled and the channel was tested by flowing deionized (DI) water through to ensure that the channel was sealed tight.

4.2 Analysis of the Performance

Once the AAO sample was made into a flow cell, I attempted to measure the AAO sample with a broadband light as the source. Before measuring the sample, I measured a blank acrylic as a reference since the AAO sample has the acrylic window as the base.

Next, I measured the flow cell with the AAO sample. This was done with no liquid in the flow cell. After that, I analyzed the images taken and divided the measured sample by the reference. As we can observe in Figure 4-4 below, the result is very similar with the OceanOptics spectrometer. Once this was confirmed, I proceeded to doing several sensing experiments using the AAO flow cell that I made.

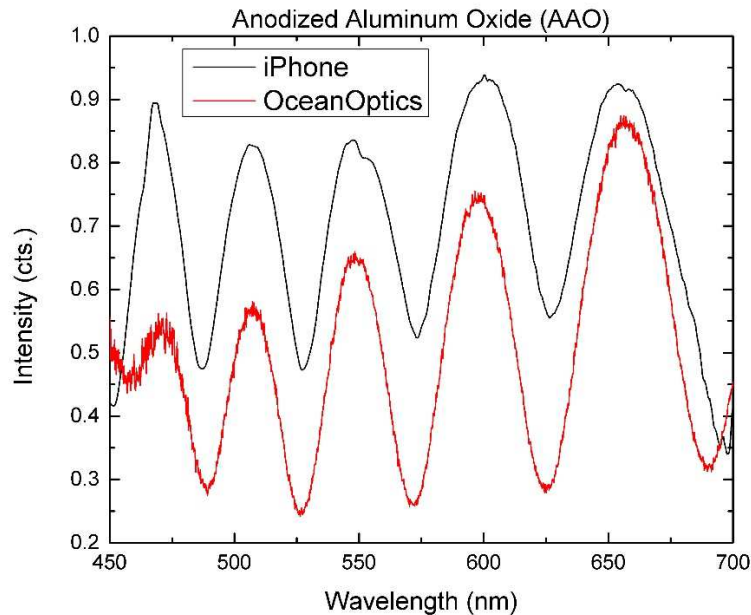


Figure 4-4: AAO spectrum measured with smartphone and OceanOptics

4.3 Sensing Experiments

In this section, I will introduce the experiments that were done with the smartphone-based spectrometer. Before proceeding to using the AAO sample, I first tested the spectrometer using a photonic crystal sample. The reason why photonic crystal was chosen to be a sample first is because of its unique signature peak. This is very apparent for photonic crystals as there is usually only one sharp peak (when measuring reflectance). A polarizer was used in order to only a certain wave of polarization to pass through.

The first experiment was done by using a photonic crystal (PC) that was deposited on a glass slide as a sample. Similar to the AAO sample, I made the photonic crystal sample into a flow cell so that I could flow liquid through the photonic crystal for testing. I conducted the experiment by flowing different concentrations of Dimethyl Sulfoxide (DMSO) through the PC flow cell. DI water was used as a reference and then the six different concentrations of DMSO solution (1%, 5% 10% and 20%) were flowed through the PC sensor respectively. The different concentrations of DMSO was a mixture of DMSO with DI water. Between each measurement of DMSO solution, the channel was rinsed with DI water to remove excess DMSO.

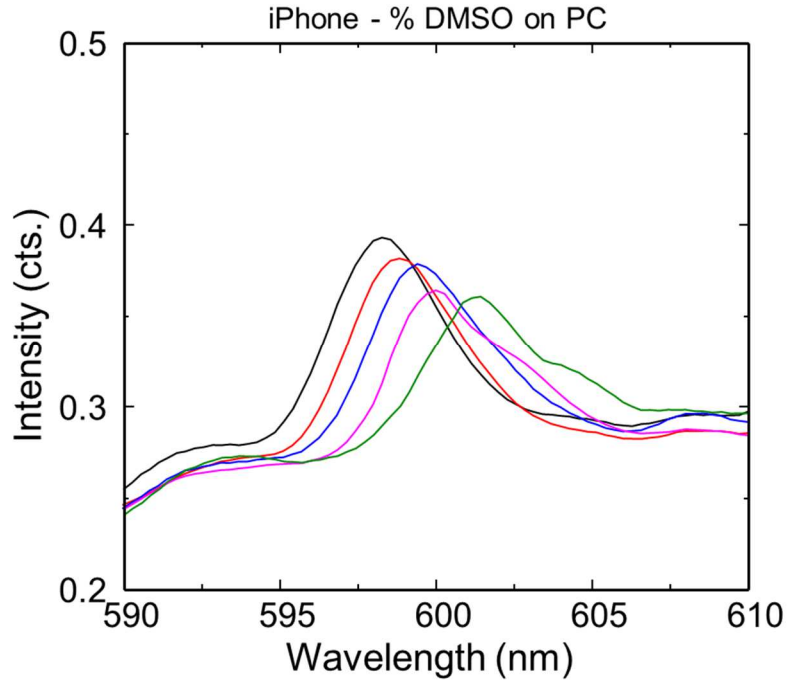


Figure 4-5: % DMSO concentration on Photonic Crystal

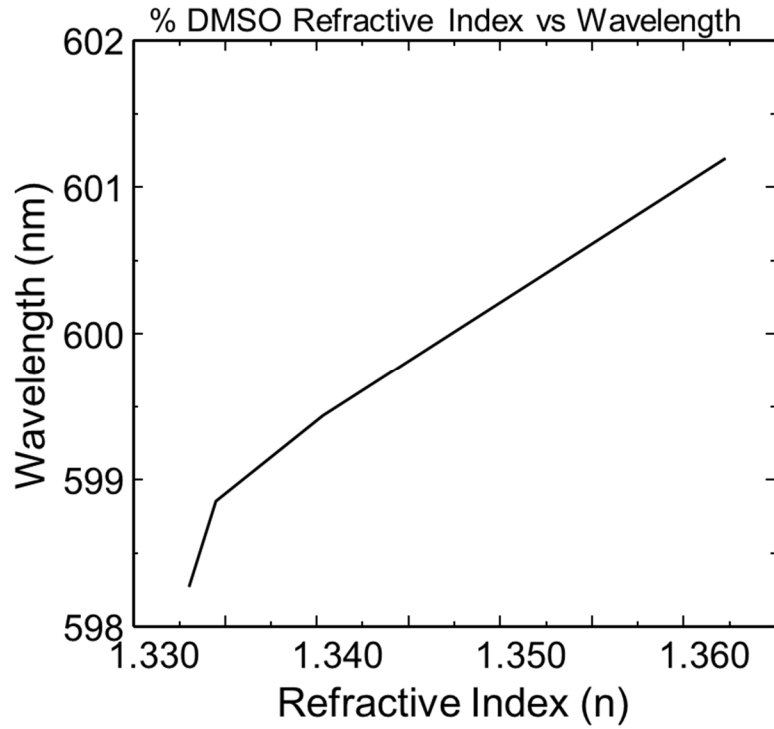


Figure 4-6: Wavelength shift based on Refractive Index

As shown in Figure 4-5 we observe that as the concentration of DMSO increases, the wavelength shifts towards the right, which is a longer wavelength. The reason is because DI water has a refractive index of 1.34 and DMSO has a refractive index of 1.4793. Therefore, the peak will continue to shift towards the right, increasing in wavelength, until the concentration of the solution is 100% DMSO where we know that the refractive index will be 1.4793. This can be observed more clearly in Figure 4-5 where the wavelength shift is plotted against the increasing refractive index. We can see that the wavelength is continuously increasing as there is an increase change in refractive index.

Next, I tested the photonic crystal sample with different polyelectrolytes. Three different polyelectrolyte solutions, Polyethylenimine (PEI), Polystyrene Sulfonic acid (PSS), and Polyallylamine Hydrochloride (PAH), were made by dissolving each polyelectrolyte with 0.9 M Sodium Chloride (NaCl) buffer at a concentration of 5mg/mL. Before building up the stacked layers, the flow cell was rinsed with the NaCl buffer for 5 minutes to establish a baseline, which is negatively charged. Then, a cationic PEI layer was placed on top of the NaCl buffer layer. After incubation for 5 minutes, the channel was washed with NaCl buffer and alternating layers of anionic PSS and cationic PAH were pushed through the flow cell. Each measurement recording was taken after the flow cell had been washed with NaCl buffer to remove excess electrolyte charges that

did not bind with the previous layer. This was repeated several times in order to observe that the layers were stacking on top of one another.



Figure 4-7: Schematic of Polyelectrolyte Layers

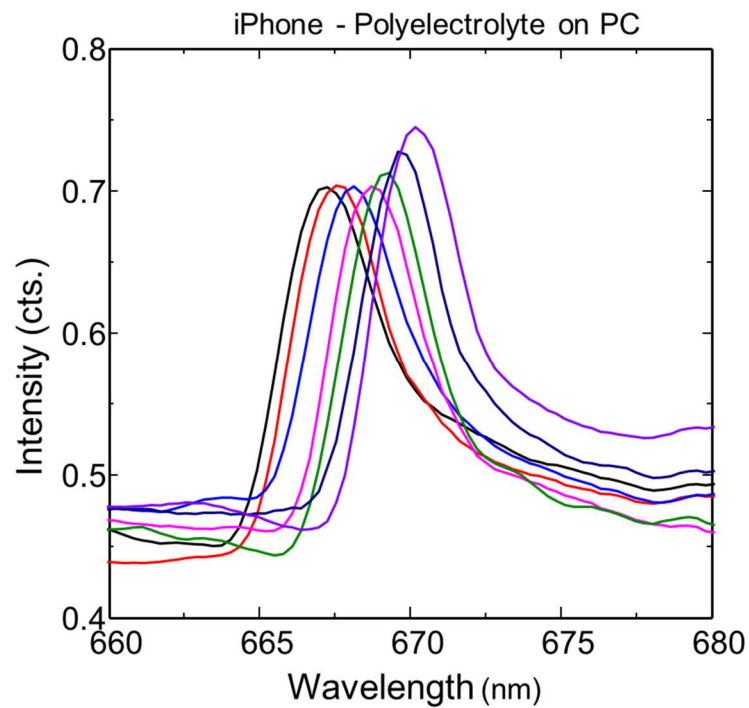


Figure 4-8: Polyelectrolyte layers on Photonic Crystal

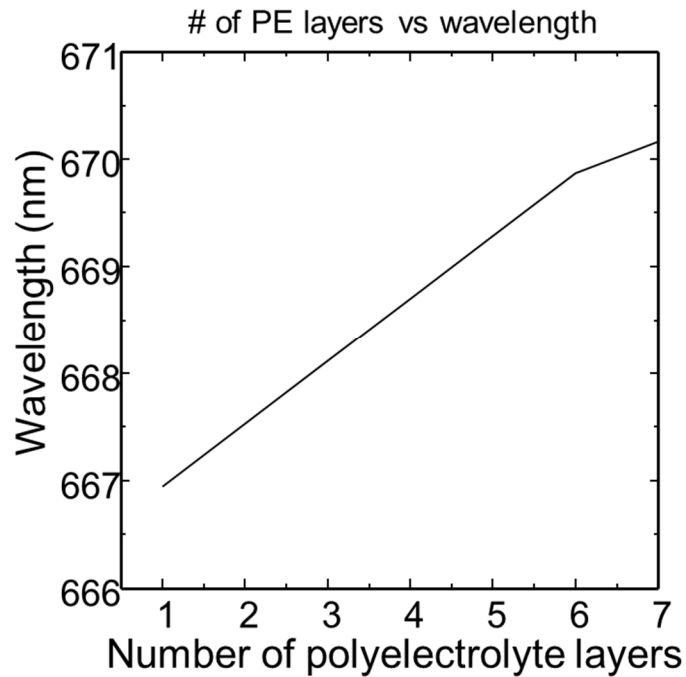


Figure 4-9: Wavelength peak shift as layers increases

In Figure 4-7, we observe that as the layers of polyelectrolyte stack up on each other. It starts with a layer of PEI, which is negatively charged, then the next layer would be PSS where it is positively charged. This repeats with different charges stacking on top of one another. In Figure 4-8, the peak in the photonic crystal gradually shifts towards the right. The reason for that is because as each layer stacks on top of the other, the refractive index changes thus causing the shift. As the number of layers increase, the refractive index increases as well. In Figure 4-7, we can see that since there is a different charge on each layer, the layers are stacked on top of each other when left for incubation. In order to observe better, the wavelength is plotted against number of

polyelectrolyte layers. Here, we are able to observe that the wavelength is definitely increasing as the polyelectrolyte layers increase.

Now that it was certain that the smartphone-based spectrometer was able to detect and provide reliable results with the photonic crystal. The next step was to use the AAO sample that was provided by our collaborators.

The polyelectrolyte experiment was repeated once again using the AAO sample. The same steps were repeated as explained above when testing with the PC sample. However, since the AAO is a broad range wavelength sensor that does not have a signature peak or dip, the results looked less defined compared to PC sample. This can be observed in the graphs (Figure 4-9 & Figure 4-10) below.

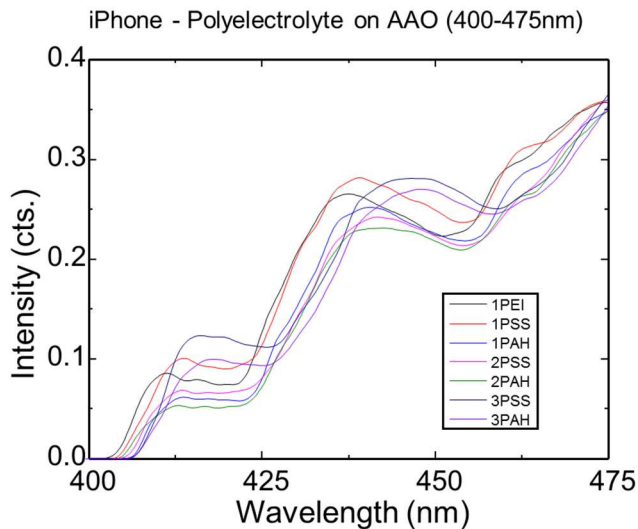


Figure 4-10: Polyelectrolyte layers on AAO (400nm-475nm)

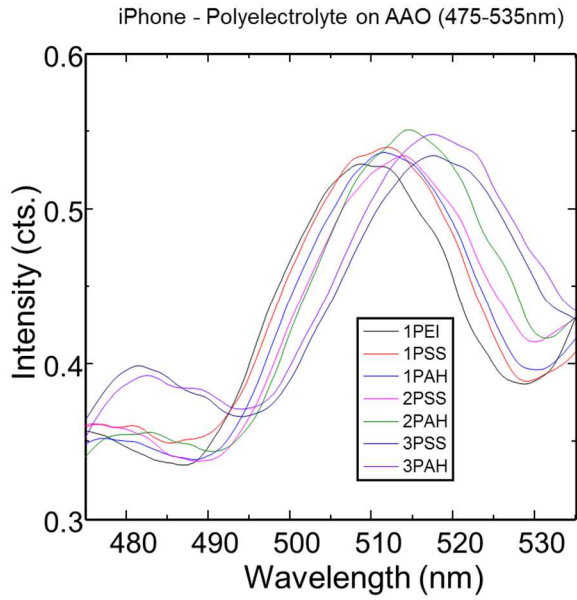


Figure 4-11: Polyelectrolyte layers on AAO (475nm-535nm)

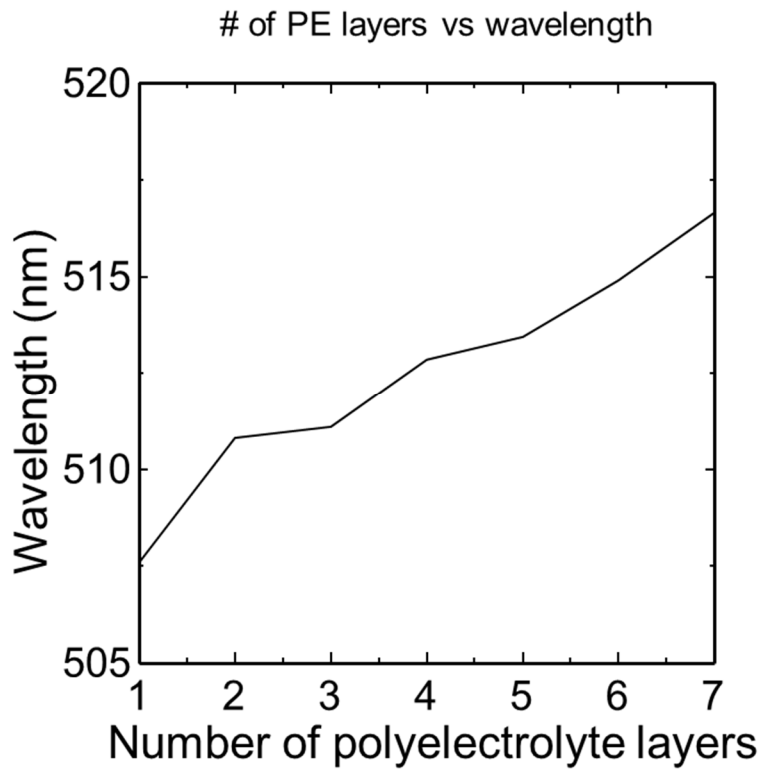


Figure 4-12: Wavelength shift with stacked polyelectrolyte layers

Although the interference patterns are not as obvious as the PC sample, we are still able to see the shift in peak wavelength that we were expecting. In order to show that this is true, the wavelength shift was plotted against the number of polyelectrolyte layers. When identifying the peaks of each layer, it is observed that the peaks still increase in wavelength as the layers stack. This can be observed in the graph (Figure 4-11) above.

Next, a polypeptide test was conducted for the AAO sample. This experiment was really straight forward. First, the channel was rinse with Phosphate-buffered saline (PBS) solution. This is a buffer solution and acted as the base for this experiment. The PBS solution was left for about 3-5 minutes to incubate. Next, the polypeptide (PPL) solution was flowed through the AAO flow cell. As soon as the PPL was flowed through the flow cell, an image was taken every five seconds because the shift of wavelength peak would be very quick. The PPL solution was left to incubate for five minutes. Since I did not know when the peak would shift, I made sure to continuously take a picture every five seconds for five minutes. Once the five minutes are up, the flow cell was rinse with PBS and measurements were taken.

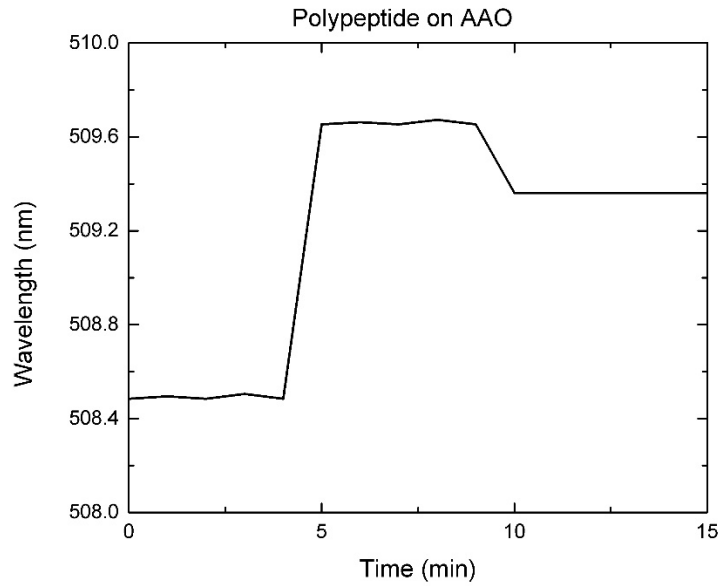


Figure 4-13: Polypeptide on AAO sample

As observed in the figure above, we can see that at minute 0, the peak stays at 508.4nm. This goes on for 5 minutes. As soon as the polypeptide solution is flowed through the flow cell, the change is very apparent and drastic. It immediately shifts to 509.6nm. The polypeptide is left to incubate for 5 minutes and we can observe that the peak stayed constant at 509.6nm. After that, the flow cell that was incubating the polypeptide solution shows that there is no change, PBS was flowed through. We can observe a slight dip in figure above which shows that the peak has shifted backwards in wavelength, moving to approximately 509.4nm. The reason for this occurring is because the excess polypeptide that did not bind with the AAO surface has been washed away and thus the refractive index changed to a smaller index.

CHAPTER 5 : SMARTPHONE-BASED FLUORESCENCE POLARIZATION SENSOR

5.1 Background of Fluorescence Polarization Assay

The theory of fluorescence polarization was first coined in 1926 by Perrin, where it is based on the observation that the fluorescent molecules in a solution, if excited by a plane-polarized light, will then emit light back onto a fixed plane. This only occurs if the molecules remain stationary during the excitation of the fluorophore. However, molecules rotate and tumble which can cause the plane in which the light is emitted to be different from the plane used for the initial excitation.

The principle is that when a fluorescent molecule is excited with a plane-polarized light, light will be emitted in the same polarized plane if and only if the molecule is stationary throughout the excited state. However, if a molecule rotates during that time and tumbles out, light will be emitted in a different plane from the initial excitation light. When vertically polarized light is excited the fluorophore, the intensity of the light can be monitored in both the horizontal and vertical planes. Thus, if a molecule is very large, very little movement occurs during excitation and this causes the emitted light to remain highly polarized. On the other hand, if a molecule is small, the rotation is much faster which would cause the molecule to tumble out and the emitted light would be depolarized.

With this, we proceeded to attempt to create a very compact and small fluorescence polarization sensor. In the next section, I will be explaining how I started creating the sensor from scratch.

5.2 Design of the Compact Instrument

In this section, I will start to introduce the schematic of the fluorescence polarization sensor where it was first discussed with Prof. Lu to sketching it up on Solidworks and 3D printing it. Then, I will briefly show the end result of the sensor.

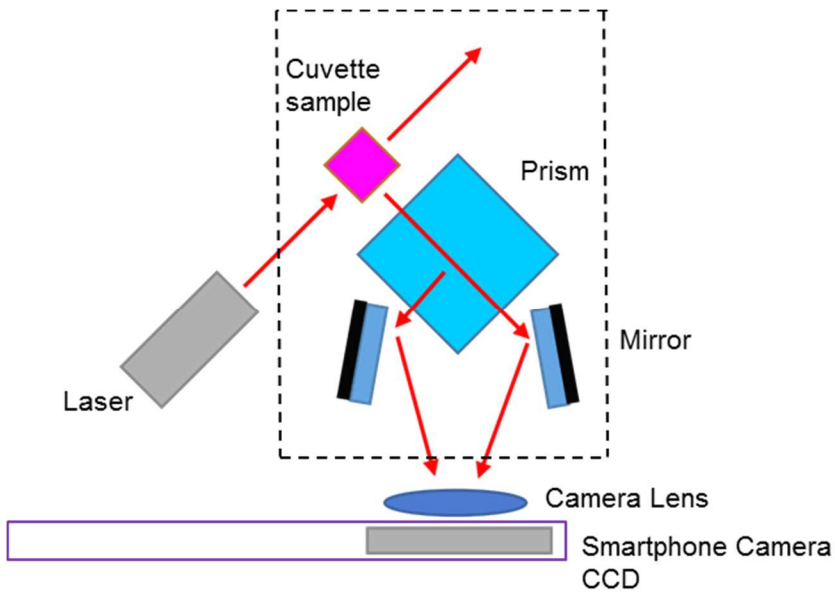


Figure 5-1: Schematic for Fluorescence Polarization Sensor. Light emission from a laser enters the fluorescence polarization sensor. The light shines onto the cuvette sample and is reflected onto the beamsplitter prism where the horizontal and vertical polarization is split into directions and is reflected onto the camera lens via mirrors.

The fluorescence polarization sensor consists of several different components. First, a light source which would most probably be a laser. Next, we have a polarizing beamsplitter cube that would split and direct the different polarized light through different a different light path as shown in Figure 5-1. After that, we have 2 mirrors that

would reflect and direct the 2 different polarizations onto the smartphone camera lens. This would appear as two pictures mirroring one another.

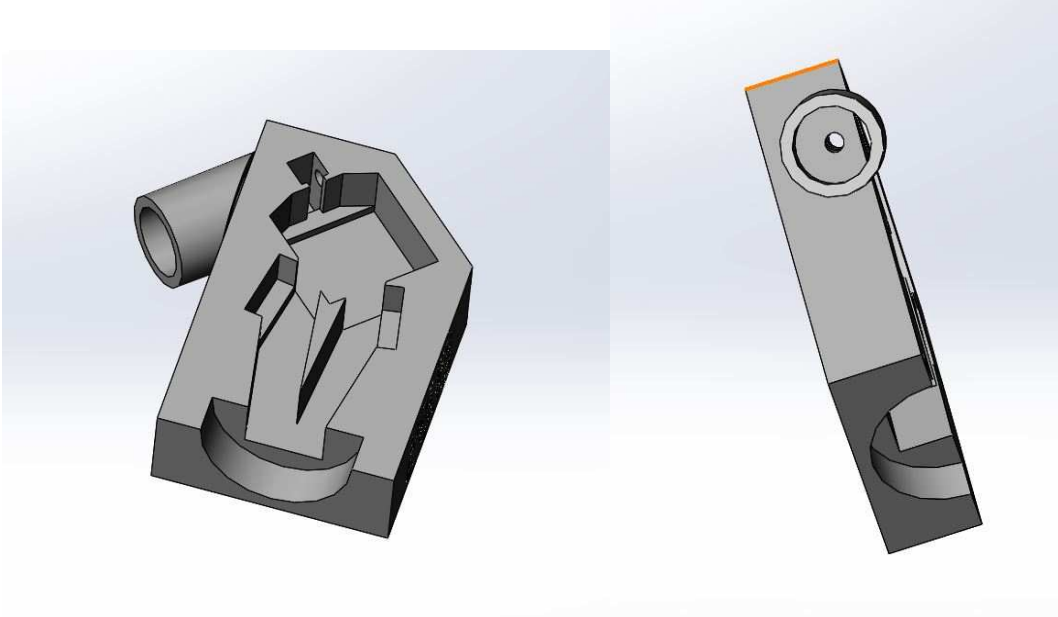


Figure 5-2: Top view

Figure 5-3: Side view

The two figures above simply show the sketch of the fluorescence polarization sensor in Solidworks. In the first figure (figure 5-2), the two small mirrors that will reflect the light are set at an angle of 55° . This was done so that the both the light of different polarization would reflect right onto the camera CCD. In figure 5-3, this is the view of where the laser would be plugged into. This was made so that the light beam would not be moving and be able to provide a good light intensity.

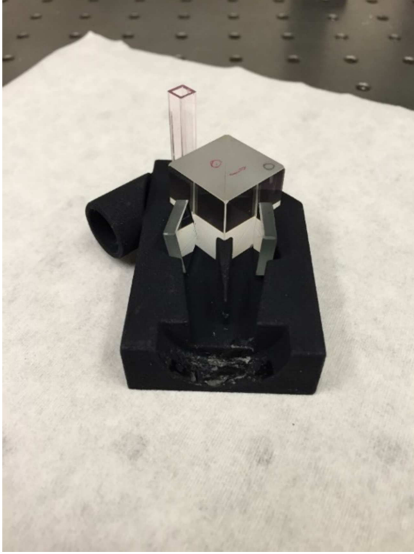


Figure 5-4: 3D-printed Fluorescence Polarization Sensor

The picture above shows the 3D printed version of the fluorescence polarization sensor. As you can observe, the mirrors fit perfectly and it came out compact. Now that this was done, let us take a look how an image taken from the smartphone would look like.

5.3 Results

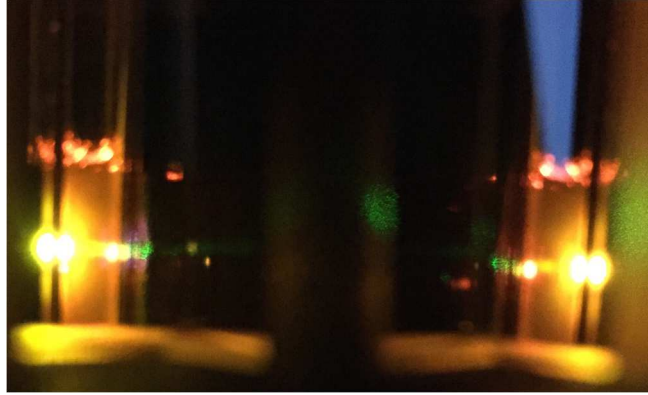


Figure 5-5: Fluorescence Polarization Sensor Image

Figure 5-5 shows a test image of how the sensor would look like when testing experiments are done. This is simply an image of a laser illuminating a fluorescence solution where the two different polarizations are captured and as explained in the earlier section, mirrored to one another.

CHAPTER 6 : CONCLUSIONS

6.1 Conclusion of Research Work

In this study, many different steps had to be done in order to obtain a working spectrometer. Therefore, after several designs, characterizations and experiments, a smartphone-based spectrometer was accomplished and proved to be successful. Besides that, this smartphone-based spectrometer has also proven to be robust and quite affordable. More importantly, the design of the reflectance-based spectrometer is very compact and has the potential to be even more compact. This has made the smartphone-based spectrometer very portable as well. I certainly hope that this spectrometer will have improved further in the future and will be able to provide help to developing countries.

As we review the sensing experiment results, the photonic crystal sample seems to be clearer due to the signature of photonic crystals. The signature wavelength was detected and the results great. The PC sensor results were compared to the Ocean Optics spectrometer and based on results, the smartphone-based spectrometer has proven to be very similar to the USB4000.

Next, the AAO sensor is a broad wavelength sensor and there is no signature wavelength to be observed. Therefore, the results were not as defined as they were with the photonic crystal. Despite that, the shift in wavelength was apparent enough that a peak could be determined.

6.2 Suggestions of Future Work

There are several suggestions for future work regarding the smartphone-based spectrometer and fluorescence polarization sensor. Firstly, I believe that the smartphone-based spectrometer can be further improved by integrating the light source and also a sample holder with the spectrometer. This can be an attachment or an add-on or fully integrated with the spectrometer.

Next, I believe that the Bayer filter is able to be fixed. In order to do so, it may require some intense calculations. However, I do believe that once that is fixed, the spectrum graph would look much better and perhaps it will improve previous measurements too. As for the fluorescence polarization sensor, I believe that characterization and testing would need to be done. This sensor would be really useful for measuring all kinds of biomarkers and advancement of mobile health technology for developing countries.

APPENDIX. PUBLICATIONS

[1] Benjamin Ch'ng, Yilun Ji, Meng Lu "Development of Smartphone-based Spectroscopy Instruments for Diagnostic Test Analysis" (Pending Applied Optics)

[2] Sol-Gel Imprint Lithography for Guided Mode Resonance Structures, Yin Huang, Longju Liu, Benjamin Ch'ng, Meng Lu, 2015 IEEE Photonics conference, Reston, Virginia USA

BIBLIOGRAPHY

- [1] Agilent.com,. 2015. 'Agilent | Agilent 101: Intro To Optical Spectroscopy'.
http://www.agilent.com/labs/features/2011_101_spectroscopy.html.
- [2] Boulos, Maged, Steve Wheeler, Carlos Tavares, and Ray Jones. 2011. 'How Smartphones Are Changing The Face Of Mobile And Participatory Healthcare: An Overview, With Example From Ecaalyx'. *Biomedical Engineering Online* 10 (1): 24. doi:10.1186/1475-925x-10-24.
- [3] Gallegos, Dustin, Kenneth D. Long, Hojeong Yu, Peter P. Clark, Yixiao Lin, Sherine George, Pabitra Nath, and Brian T. Cunningham. 2013. 'Label-Free Biodetection Using A Smartphone'. *Lab On A Chip* 13 (11): 2124. doi:10.1039/c3lc40991k.
- [4] Liu, Xiong, Qiu Dai, Lauren Austin, Janelle Coutts, Genevieve Knowles, Jianhua Zou, Hui Chen, and Qun Huo. 2008. 'A One-Step Homogeneous Immunoassay For Cancer Biomarker Detection Using Gold Nanoparticle Probes Coupled With Dynamic Light Scattering'. *J. Am. Chem. Soc.* 130 (9): 2780-2782. doi:10.1021/ja711298b.
- [5] Long, Kenneth D., Hojeong Yu, and Brian T. Cunningham. 2014. 'Smartphone Instrument For Portable Enzyme- Linked Immunosorbent Assays'. *Biomedical Optics Express* 5 (11): 3792. doi:10.1364/boe.5.003792.

- [6] Mhealthknowledge.org,. 2015. 'Five Years Of Mobilizing For Health Impact: Key Achievements And Future Opportunities | Wwww.Mhealthknowledge.Org'.
<http://www.mhealthknowledge.org/resources/five-years-mobilizing-health-impact-key-achievements-and-future-opportunities>.
- [7] Moerner, W. E., and L. Kador. 1989. 'Optical Detection And Spectroscopy Of Single Molecules In A Solid'. *Phys. Rev. Lett.* 62 (21): 2535-2538.
doi:10.1103/physrevlett.62.2535.
- [8] MOERNER, W. E., and T. BASCHE. 1993. 'Cheminform Abstract: Optical Spectroscopy Of Single Impurity Molecules In Solids'. *Cheminform* 24 (29): no-no.
doi:10.1002/chin.199329350.
- [9] Vasan, R. S. 2006. 'Biomarkers Of Cardiovascular Disease: Molecular Basis And Practical Considerations'. *Circulation* 113 (19): 2335-2362.
doi:10.1161/circulationaha.104.482570.
- [10] Wang, X. F, and Brian Herman. 1996. *Fluorescence Imaging Spectroscopy And Microscopy*. New York: Wiley.
- [11]Wei, Qingshan, Richie Nagi, Kayvon Sadeghi, Steve Feng, Eddie Yan, So Jung Ki, Romain Caire, Derek Tseng, and Aydogan Ozcan. 2014. 'Detection And Spatial Mapping Of Mercury Contamination In Water Samples Using A Smart-Phone'. *ACS Nano* 8 (2): 1121-1129. doi:10.1021/nn406571t.

[12] 2015. <http://home.uni-leipzig.de/energy/pdf/freuse1.pdf>.

[13] Yu, Hojeong, Yafang Tan, and Brian T. Cunningham. 2014. 'Smartphone Fluorescence Spectroscopy'. *Analytical Chemistry* 86 (17): 8805-8813. doi:10.1021/ac502080t.